BOILING AND THE LEIDENFROST EFFECT

JEARL WALKER
Cleveland State University

How does water boil? As commonplace as the event is, you may not have noticed all of its curious features. Some of the features are important in industrial applications, while others appear to be the basis for certain dangerous stunts once performed by daredevils in carnival sideshows.

Arrange for a pan of tap water to be heated from below by a flame or electric heat source. As the water warms, air molecules are driven out of solution in the water, collecting as tiny bubbles in crevices along the bottom of the pan (Fig. 1a). The air bubbles gradually inflate, and then they begin to pinch off from the crevices and rise to the top surface of the water (Figs. 1b–f). As they leave, more air bubbles form in the crevices and pinch off, until the supply of air in the water is depleted. The formation of air bubbles is a sign that the water is heating but has nothing to do with boiling.

Water that is directly exposed to the atmosphere boils at what is sometimes called its normal boiling temperature T_S. For example, T_S is about 100°C when the air pressure is 1 atm. Since the water at the bottom of your pan is not directly exposed to the atmosphere, it remains liquid even when it *superheats* above T_S by as much as a few degrees. During this process, the water is constantly mixed by convection as hot water rises and cooler water descends.

If you continue to increase the pan's temperature, the bottom layer of water begins to vaporize, with water molecules gathering in small vapor bubbles in the now dry crevices, as the air bubbles do in Fig. 1. This phase of boiling is signaled by pops, pings, and eventually buzzing. The water
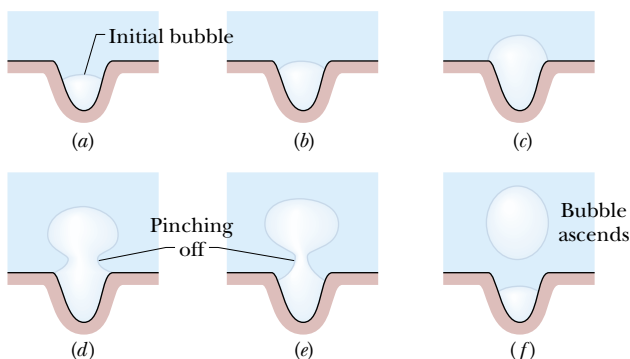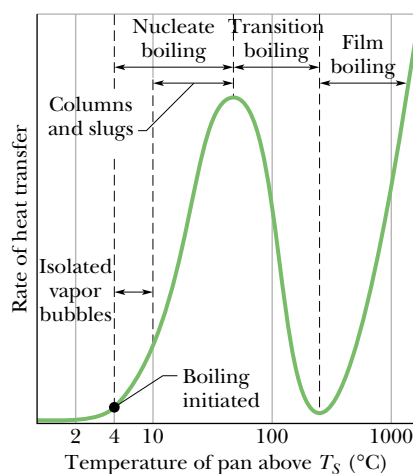

Fig. 2 Boiling curve for water. As the temperature at the bottom of the pan is increased above the normal boiling point, the rate at which energy is transferred from the pan bottom to the water increases at first. However, above a certain temperature, the transfer almost disappears. At even higher temperatures, the transfer reappears.

Fig. 1 (a) A bubble forms in the crevice of a scratch along the bottom of a pan of water. (b–f) The bubble grows, pinches off, and then ascends through the water.

almost sings its displeasure at being heated. Every time a vapor bubble expands upward into slightly cooler water, the bubble suddenly collapses because the vapor within it condenses. Each collapse sends out a sound wave, the ping you hear. Once the temperature of the bulk water increases, the bubbles may not collapse until after they pinch off from the crevices and ascend part of the way to the top surface of the water. This phase of boiling is labeled ''isolated vapor bubbles'' in Fig. 2.

If you still increase the pan's temperature, the clamor of collapsing bubbles first grows louder and then disappears. The noise begins to soften when the bulk liquid is sufficiently hot that the vapor bubbles reach the top surface of the water. There they pop open with a light splash. The water is now in full boil.

If your heat source is a kitchen stove, the story stops at this point. However, with a laboratory burner you can continue to increase the pan's temperature. The vapor bubbles next become so abundant and pinch off from their crevices so frequently that they coalesce, forming columns of vapor that violently and chaotically churn upward, sometimes meeting previously detached ''slugs'' of vapor.

The production of vapor bubbles and columns is called *nucleate boiling* because the formation and growth of the bubbles depend on crevices serving as *nucleating sites* (sites of formation). Whenever you increase the pan's temperature,

the rate at which energy is transferred as heat to the water increases. If you continue to raise the pan's temperature past the stage of columns and slugs, the boiling enters a new phase called the *transition regime.* Then each increase in the pan's temperature reduces the rate at which energy is transferred to the water. The decrease is not paradoxical. In the transition regime, much of the bottom of the pan is covered by a layer of vapor. Since water vapor conducts energy about an order of magnitude more poorly than does liquid water, the transfer of energy to the water is diminished. The hotter the pan becomes, the less direct contact the water has with it and the worse the transfer of energy becomes. This situation can be dangerous in a *heat exchanger,* whose purpose is to transfer energy from a heated object. If the water in the heat exchanger is allowed to enter the transition regime, the object may destructively overheat because of diminished transfer of energy from it.

Suppose you continue to increase the temperature of the pan. Eventually, the whole of the bottom surface is covered with vapor. Then energy is slowly transferred to the liquid above the vapor by radiation and gradual conduction. This phase is called *film boiling.*

Although you cannot obtain film boiling in a pan of water on a kitchen stove, it is still commonplace in the kitchen. My grandmother once demonstrated how it serves to indicate when her skillet is hot enough for pancake batter. After she heated the empty skillet for a while, she sprinkled a few drops of water into it. The drops sizzled away within seconds. Their rapid disappearance warned her that the skillet was insufficiently hot for the batter. After further heating the skillet, she repeated her test with a few more sprinkled water drops. This time they beaded up and danced over the metal, lasting well over a minute before they disappeared. The skillet was then hot enough for my grandmother's batter.

To study her demonstration, I arranged for a flat metal plate to be heated by a laboratory burner. While monitoring

Fig. 3 Drop lifetimes on a hot plate. Strangely, in a certain temperature range, the drops last longer when the hot plate is hotter.

the temperature of the plate with a thermocouple, I carefully released a drop of distilled water from a syringe held just above the plate. The drop fell into a dent I had made in the plate with a ball-peen hammer. The syringe allowed me to release drops of uniform size. Once a drop was released, I timed how long it survived on the plate. Afterward, I plotted the survival times of the drops versus the plate temperature (Fig. 3). The graph has a curious peak. When the plate temperature was between 100 and about 200°C, each drop spread over the plate in a thin layer and rapidly vaporized. When the plate temperature was about 200°C, a drop deposited on the plate beaded up and survived for over a minute. At even higher plate temperatures, the water beads did not survive quite as long. Similar experiments with tap water generated a graph with a flatter peak, probably because suspended particles of impurities in the drops breached the vapor layer, conducting heat into the drops.

The fact that a water drop is long lived when deposited on metal that is much hotter than the boiling temperature of water was first reported by Hermann Boerhaave in 1732. It was not investigated extensively until 1756 when Johann Gottlob Leidenfrost published ''A Tract About Some Qualities of Common Water.'' Because Leidenfrost's work was not translated from the Latin until 1965, it was not widely read. Still, his name is now associated with the phenomenon. In addition, the temperature corresponding to the peak in a graph such as I made is called the Leidenfrost point.

Leidenfrost conducted his experiments with an iron spoon that was heated red-hot in a fireplace. After placing a drop of water into the spoon, he timed its duration by the swings of a pendulum. He noted that the drop seemed to suck the light and heat from the spoon, leaving a spot duller than the rest of the spoon. The first drop deposited in the spoon lasted 30 s while the next drop lasted only 10 s. Additional drops lasted only a few seconds.

Leidenfrost misunderstood his demonstrations because he did not realize that the longer-lasting drops were actually boiling. Let me explain in terms of my experiments. When the temperature of the plate is less than the Leidenfrost point, the water spreads over the plate and rapidly conducts energy from it, resulting in complete vaporization within seconds. When the temperature is at or above the Leidenfrost point, the bottom surface of a drop deposited on the plate almost immediately vaporizes. The gas pressure from this vapor layer prevents the rest of the drop from touching the plate (Fig. 4). The layer thus protects and supports the drop for the next minute or so. The layer is constantly replenished as additional water vaporizes from the bottom surface of the drop because of energy radiated and conducted through the layer from the plate. Although the layer is less than 0.1 mm thick near its outer boundary and only about 0.2 mm thick at its center, it dramatically slows the vaporization of the drop.
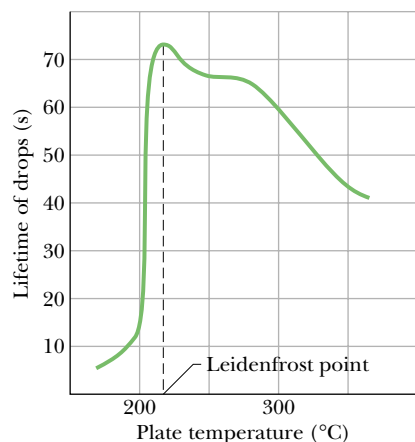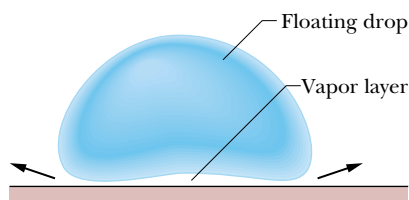
Fig. 4 A Leidenfrost drop in cross section.

After reading the translation of Leidenfrost's research, I happened upon a description of a curious stunt that was performed in the sideshows of carnivals around the turn of the century. Reportedly, a performer was able to dip wet fingers into molten lead. Assuming that the stunt involved no trickery, I conjectured that it must depend on the Leidenfrost effect. As soon as the performer's wet flesh touched the hot liquid metal, part of the water vaporized, coating the fingers with a vapor layer. If the dip was brief, the flesh would not be heated significantly.

I could not resist the temptation to test my explanation. With a laboratory burner, I melted down a sizable slab of lead in a crucible. I heated the lead until its temperature was over 400°C, well above its melting temperature of 328°C. After wetting a finger in tap water, I prepared to touch the top surface of the molten lead. I must confess that I had an assistant standing ready with first-aid materials. I must also confess that my first several attempts failed because my brain refused to allow this ridiculous experiment, always directing my finger to miss the lead.

When I finally overcame my fears and briefly touched the lead, I was amazed. I felt no heat. Just as I had guessed, part of the water on the finger vaporized, forming a protective layer. Since the contact was brief, radiation and conduction of energy through the vapor layer were insufficient to raise perceptibly the temperature of my flesh. I grew braver. After wetting my hand, I dipped all my fingers into the lead, touching the bottom of the container (Fig. 5). The contact with the lead was still too brief to result in a burn. Apparently, the Leidenfrost effect, or more exactly, the immediate presence of film boiling, protected my fingers.

I still questioned my explanation. Could I possibly touch the lead with a dry finger without suffering a burn? Leaving aside all rational thought, I tried it, immediately realizing my folly when pain raced through the finger. Later, I tested a dry wiener, forcing it into the molten lead for several seconds. The skin of the wiener quickly blackened. It lacked the protection of film boiling just as my dry finger had.

I must caution that dipping fingers into molten lead presents several serious dangers. If the lead is only slightly above its melting point, the loss of energy from it when the water is vaporized may solidify the lead around the fingers. If I were to pull the resulting glove of hot, solid lead up from the container, it will be in contact with my fingers so long that my fingers are certain to be badly burned. I must also contend with the possibility of splashing and spillage. In addition, there is the acute danger of having too much water on the fingers. When the surplus water rapidly vaporizes, it can blow molten lead over the surroundings and, most seriously, into the eyes. I have been scarred on my arms and face from such explosive vaporizations. *You should never repeat this demonstration.*

Film boiling can also be seen when liquid nitrogen is spilled. The drops and globs bead up as they skate over the floor. The liquid is at a temperature of about −200°C. When the spilled liquid nears the floor, its bottom surface vaporizes. The vapor layer then provides support for the rest of the liquid, allowing the liquid to survive for a surprisingly long time.

I was told of a stunt where a performer poured liquid nitrogen into his mouth without being hurt by its extreme cold. The liquid immediately underwent film boiling on its bottom surface and thus did not directly touch the tongue. Foolishly, I repeated this demonstration. For several dozen times the stunt went smoothly and dramatically. With a large glob of liquid nitrogen in my mouth, I concentrated on not

Fig. 5 Walker demonstrating the Leidenfrost effect with molten lead. He has just plunged his fingers into the lead, touching the bottom of the pan. The temperature of the lead is given in degrees Fahrenheit on the industrial thermometer.

swallowing while I breathed outward. The moisture in my cold breath condensed, creating a terrific plume that extended about a meter from my mouth. However, on my last attempt the liquid thermally contracted two of my front teeth so severely that the enamel ruptured into a ''road map'' of fissures. My dentist convinced me to drop the demonstration.

The Leidenfrost effect may also play a role in another foolhardy demonstration: walking over hot coals. At times the news media have carried reports of a performer striding over red-hot coals with much hoopla and mystic nonsense, perhaps claiming that protection from a bad burn is afforded by ''mind over matter.'' Actually, physics protects the feet when the walk is successful. Particularly important is the fact that although the surface of the coals is quite hot, it contains surprisingly little energy. If the performer walks at a moderate pace, a footfall is so brief that the foot conducts little energy from the coals. Of course, a slower walk invites a burn because the longer contact allows energy to be conducted to the foot from the interior of the coals.

If the feet are wet prior to the walk, the liquid might also help protect them. To wet the feet a performer might walk over wet grass just before reaching the hot coals. Instead, the feet might just be sweaty because of the heat from the coals or the excitement of the performance. Once the performer is on the coals, some of the heat vaporizes the liquid on the feet, leaving less energy to be conducted to the flesh. In addition, there may be points of contact where the liquid undergoes film boiling, thereby providing brief protection from the coals.

I have walked over hot coals on five occasions. For four of the walks I was fearful enough that my feet were sweaty. However, on the fifth walk I took my safety so much for granted that my feet were dry. The burns I suffered then were extensive and terribly painful. My feet did not heal for weeks.

My failure may have been due to a lack of film boiling on the feet, but I had also neglected an additional safety factor. On the other days I had taken the precaution of clutching an early edition of *Fundamentals of Physics* to my chest during the walks so as to bolster my belief in physics. Alas, I forgot the book on the day when I was so badly burned.

I have long argued that degree-granting programs should employ ''fire-walking'' as a last exam. The chairperson of the program should wait on the far side of a bed of red-hot coals while a degree candidate is forced to walk over the coals. If the candidate's belief in physics is strong enough that the feet are left undamaged, the chairperson hands the candidate a graduation certificate. The test would be more revealing than traditional final exams.

References

Leidenfrost, Johann Gottlob, ''On the Fixation of Water in Diverse Fire,'' *International Journal of Heat and Mass Transfer,* Vol. 9, pages 1153–1166 (1966).

Gottfried, B. S., C. J. Lee, and K. J. Bell, ''The Leidenfrost Phenomenon: Film Boiling of Liquid Droplets on a Flat Plate,'' *International Journal of Heat and Mass Transfer,* Vol. 9, pages 1167–1187 (1966).

Hall, R. S., S. J. Board, A. J. Clare, R. B. Duffey, T. S. Playle, and D. H. Poole, ''Inverse Leidenfrost Phenomenon,'' *Nature,* Vol. 224, pages 266–267 (1969).

Walker, Jearl, ''The Amateur Scientist,'' *Scientific American,* Vol. 237, pages 126–131, 140 (August 1977).

Curzon, F. L., ''The Leidenfrost Phenomenon,'' *American Journal of Physics,* Vol. 46, pages 825–828 (1978).

Leikind, Bernard J., and William J. McCarthy, ''An Investigation of Firewalking,'' *Skeptical Inquirer,* Vol. 10, No. 1, pages 23–34 (Fall 1985).

Bent, Henry A., ''Droplet on a Hot Metal Spoon,'' *American Journal of Physics,* Vol. 54, page 967 (1986).

Leikind, B. J., and W. J. McCarthy, ''Firewalking,'' *Experientia,* Vol. 44, pages 310–315 (1988).

Thimbleby, Harold, ''The Leidenfrost Phenomenon,'' *Physics Education,* Vol. 24, pages 300–303 (1989).

Taylor, John R., ''Firewalking: A Lesson in Physics,'' *The Physics Teacher,* Vol. 27, pages 166–168 (March 1989).

Zhang, S., and G. Gogos, ''Film Evaporation of a Spherical Droplet over a Hot Surface: Fluid Mechanics and Heat/Mass Transfer Analysis,'' *Journal of Fluid Mechanics,* Vol. 222, pages 543–563 (1991).

Agrawal, D. C., and V. J. Menon, ''Boiling and the Leidenfrost Effect in a Gravity-free Zone: A Speculation,'' *Physics Education,* Vol. 29, pages 39–42 (1994).

A boiling heat transfer paradox

G. Guido Lavalle, P. Carrica, V. Garea, and M. Jaime

Related Articles

Additional information on Am. J. Phys.

J. D. Bernardin

Research Engineer,
Los Alamos National Laboratory

I. Mudawar

Professor and Director

Boiling and Two-Phase Flow Laboratory,
School of Mechanical Engineering,
Purdue University,
West Lafayette, IN 47907

The Leidenfrost Point: Experimental Study and Assessment of Existing Models

This study presents a detailed and thorough parametric study of the Leidenfrost point (LFP), which serves as the temperature boundary between the transition and film boiling regimes. Sessile drop evaporation experiments were conducted with acetone, benzene, FC-72, and water on heated aluminum surfaces with either polished, particle blasted, or rough sanded finishes to observe the influential effects of fluid properties, surface roughness, and surface contamination on the LFP. A weak relationship between surface energies and the LFP was observed by performing droplet evaporation experiments with water on polished copper, nickel, and silver surfaces. Additional parameters which were investigated and found to have negligible influence on the LFP included liquid subcooling, liquid degassing, surface roughness on the polished level, and the presence of polishing paste residues. The accumulated LFP data of this study was used to assess several existing models which attempt to identify the mechanisms which govern the LFP. The disagreement between the experimental LFP values and those predicted by the various models suggests that an accurate and robust theoretical model which effectively captures the LFP mechanisms is currently unavailable.

1 Introduction

Recent demands for superior material properties and more efficient use of materials and production time are forcing manufacturers to develop intelligent processing techniques for enhanced process control in order to better dictate the end product. In the heat treatment and processing of metallic alloys, the desire to obtain parts of enhanced and uniform mechanical properties is requiring increased control over heat removal rates and enhanced temperature control. In particular, spray quenching has been shown (Bernardin and Mudawar, 1995) to be an effective means to control and enhance the cooling rates of heat treatable aluminum alloys. Rapid quenching is required to obtain high material strength, while uniform temperature control is necessary to reduce warping and deformation. In addition, the quench rate and material properties of aluminum alloys following solution heat treatment are dictated mainly by low heat flux, high-temperature film boiling spray heat transfer, and the Leidenfrost point (LFP) which forms the lower temperature limit of the film boiling regime (Bernardin, 1993). Thus, when quenching most aluminum alloys, it is desirable to traverse through the film boiling temperature range and get below the LFP as quickly as possible. Consequently, accurate knowledge of the Leidenfrost temperature is necessary if accurate and enhanced control of the quenching process and resulting material properties is desired.

A common technique used for determining the Leidenfrost temperature requires measuring evaporation times of liquid sessile droplets of a given initial volume over a range of surface temperatures to produce a droplet evaporation curve as shown in Fig. 1(b). The curve displays droplet evaporation lifetime versus surface temperature and exhibits the four distinct heat transfer regimes shown on the traditional pool boiling curve of Fig. 1(a). In the single-phase regime, characterized by long evaporation times, heat from the surface is conducted through the liquid film and is dissipated by evaporation at the liquid-gas interface. In the nucleate boiling regime, vapor bubble production and the corresponding

heat flux increase dramatically, thus decreasing the droplet lifetime. The upper limit of the nucleate boiling regime, known as critical heat flux (CHF), corresponds to a maximum heat flux and minimum drop lifetime. In the transition regime, a noncontinuous, insulating vapor layer develops beneath portions of the droplet, leading to reduced evaporation rates and increased drop lifetime. At the upper end of the transition boiling regime, referred to as the LFP, the vapor layer grows substantially to prevent any significant contact between the drop and surface and the droplet evaporation time reaches a maximum. At surface temperatures above the LFP, the droplet remains separated from the surface by a thin vapor layer through which heat is conducted.

Literature Review and Focus of Current Study. Table 1 displays the large variations in the Leidenfrost temperature for water which have been reported in the literature. The discrepancies in these reported values arise from differences in size of the liquid mass, method of liquid deposition, amount of liquid subcooling, solid thermal properties, surface material and finish, pressure, and presence of impurities. These parameters and their observed effects on the LFP are summarized in Table 2 along with the corresponding references.

While many of the LFP investigations have been qualitative in nature, several studies have reported various correlations for predicting the Leidenfrost temperature. One of the correlations most frequently referred to is a semi-empirical expression developed by Baumeister and Simon (1973). Adapting the superheat limit model of Spiegler et al. (1963), Baumeister and Simon included corrections to account for the thermal properties of the heated surface and wetting characteristics of the liquid-solid system, and arrived at the following semi-empirical expression:

$$T_{\text{leid,meas}} = T_f$$
$$+ \frac{0.844 T_c \left\{ 1 - \exp\left(-0.016 \left[\frac{\left(\frac{\rho_s}{At}\right)^{1.33}}{\sigma_f} \right]^{0.5} \right) \right\} - T_f}{\exp(3.066 \times 10^6 \beta) \, \text{erfc} \, (1758 \sqrt{\beta})}, \quad (1)$$
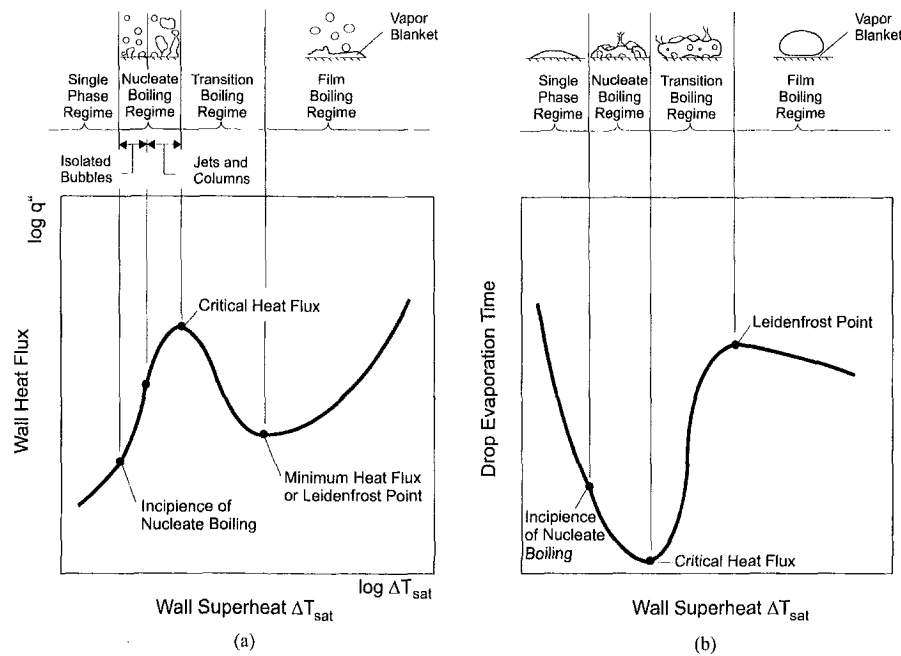
where

Fig. 1 (*a*) Boiling curve for a hot surface in a stagnant bath of liquid at saturation temperature and (*b*) sessile drop evaporation curve

$$\beta = \frac{1}{k_s \rho_s c_{p,s}}. \tag{2}$$

The temperature generally measured and reported as the LFP corresponds to that of the solid in the near vicinity of the surface. To be more precise, it is better practice to associate the LFP with the temperature of the liquid-solid interface, which is often several degrees less than that measured within the solid. It is commonly accepted that during the initial stages of droplet-surface contact, the interface temperature between the liquid and solid is dictated by the thermal properties of the liquid and solid as well as by their initial temperatures. This interface temperature, T_i, is given by the solution to the one-dimensional energy equation with semi-infinite body boundary conditions (Eckert and Drake, 1972)

$$T_i = \frac{(k \rho c_p)_s^{0.5} T_{s,o} + (k \rho c_p)_f^{0.5} T_{f,o}}{(k \rho c_p)_s^{0.5} + (k \rho c_p)_f^{0.5}}. \tag{3}$$

The first objective of this study is to present previously developed models that attempt to describe the governing LFP mechanisms. Next, experimental LFP data for several different liquid-solid systems from the current study will be used to assess these models to display their weaknesses. Based upon lack of experimental validation and sound scientific arguments, a need for a correct and robust theoretical model that correctly captures the LFP mechanisms will be identified.

2 Previous LFP Models

This section discusses several of the most commonly proposed mechanisms for the LFP for droplets and the minimum film boiling point for pools of liquid. Table 3 contains a pictorial summary and corresponding correlations associated with the various models.

Hydrodynamic Instability Hypotheses. Several authors (Zuber, 1958; Berenson, 1961; Hosler and Westwater, 1962; Yao and

---

Nomenclature

At = atomic weight of surface material
c_p = specific heat with constant pressure
d = droplet diameter
g = gravitational constant
h = enthalpy
h'_{fg} = modified latent heat of vaporization = $c_p(T_f - T_{sat}) + h_{fg}$
J = vapor embryo formation rate per unit volume of liquid
k = thermal conductivity
k_b = Boltzmann constant
M = molecular weight, constant
m = mass of a single molecule
N = number of liquid molecules per unit volume
Na = Avogadro's number
P = pressure

Q_a = heat of adsorption
R = particular gas constant, drop, film, or bubble radius
T = temperature
u = droplet velocity
v = specific volume, velocity

Greek Symbols

β = surface thermal parameter $(k \rho c_p)^{-1}$
Γ = number of monolayer surface adsorption sites
η = parameter for embryo formation rate equation
λ = wavelength
μ = dynamic viscosity
θ = contact angle
ρ = density
σ = surface tension

τ_o = molecule residence time on surface

Subscripts

c = critical
f = liquid
fg = difference between liquid and vapor
g = vapor
i = interface
leid = Leidenfrost point
mfb = minimum film boiling point
o = initial
r = reduced property
s = surface, wall
sat = saturation
thn = thermodynamic homogeneous nucleation limit

Table 1 Summary of Leidenfrost temperatures for water ($P = 101.3$ kPa) as reported in the literature

Reference	T_{leid} (°C)	Surface Material	Notes
Blaszkowska and Zakrzewka (1930)	157	Silver	
Borishansky and Kutateladze (1947)[†]	310 255	Graphite	$T_f = 20$ °C $T_f = 85$ °C
Borishansky (1953)[†]	222 194 250 237	Brass Brass Copper Copper	$T_f = 19$ °C $T_f = 89$ °C $T_f = 20$ °C $T_f = 85$ °C $d_o = 4.5$ mm
Tamura and Tanasawa (1959)	302	Stainless steel	
Gottfried (1962)[†]	285	Stainless steel	$T_f = 25$ °C $3.7 < d_o < 4.3$
Betta (1963)[††]	245	Not given	$4.6 < d_o$
Lee (1965)[††]	280	Not given	$7.8 < d_o$
Godleski and Bell (1966)	320	Stainless steel	$T_{leid} = 264$ °C for extended liquid masses and 161 °C for transient technique
Gottfried et al. (1966)	280	Stainless steel	
Kutateladze and Borishanski (1966)	250	Not given	
Patel and Bell (1966)	305	Stainless steel	$0.05 < V < 10$ ml extended masses
Baumeister et al. (1970)	515 305, 325 230, 235 >200 235 155 265 <184	Pyrex (3-4 rms) Stainless steel (3-4 rms) Brass (3-4 rms) Brass fresh polish (3-4 rms) Aluminum (3-4 rms) Alum. fresh pol. (3-4 rms) Aluminum (25 rms) Gold fresh polish	$d_o = 0.39$ mm $d_o = 0.39$ & 2.25 mm $d_o = 0.39$ & 2.25 mm $d_o = 2.25$ mm $d_o = 0.39$ & 2.25 mm $d_o = 0.39$ mm $d_o = 2.25$ mm $d_o = 2.25$ mm
Emmerson (1975)	282 316 284	Stainless steel Monel Brass	LFP also given for pressures of 210, 315, 420, and 525 kPa
Xiong and Yuen (1991)	280-310	Stainless steel	

[†] As referenced from Patel and Bell (1966), [††] As referenced from Testa and Nicotra (1986)

Henry, 1978) have used a hydrodynamic stability theory by Taylor (1950) to describe the minimum film boiling temperature for pool boiling. Assuming potential flow and a sinusoidal disturbance between two fluids of different densities (the more dense on top), Taylor (1950) used a first-order perturbation analysis to show that gravity induced interfacial disturbances with wavelengths given by the following expression will be most likely to grow and disrupt the smooth horizontal interface:

$$\lambda_d = 2\pi \left[\frac{3\sigma_f}{g(\rho_f - \rho_g)} \right]^{1/2}. \qquad (4)$$

Berenson (1961) showed that the bubble spacing in film boiling was hydrodynamically controlled by a Taylor-type instability and that the presence of the corresponding vapor layer and bubble departure supported film boiling by keeping the liquid from contacting the heated surface. Berenson's analytical expression, Eq. (5), to predict the minimum film pool boiling temperature, T_{mfb}, coincides with the point at which vapor is not generated rapidly enough to sustain the Taylor waves at the liquid-vapor interface.

$$T_{mfb} = T_{sat} + 0.127 \frac{\rho_g h_{fg}}{k_g} \left[\frac{g(\rho_f - \rho_g)}{\rho_f + \rho_g} \right]^{2/3}$$
$$\times \left[\frac{\sigma}{g(\rho_f - \rho_g)} \right]^{1/2} \left[\frac{\mu_g}{g(\rho_f - \rho_g)} \right]^{1/3} \qquad (5)$$
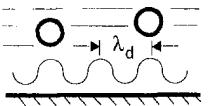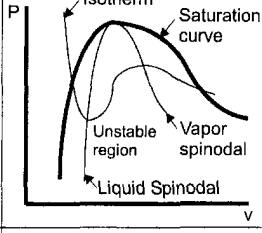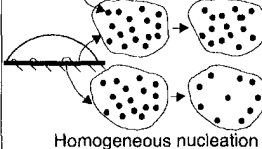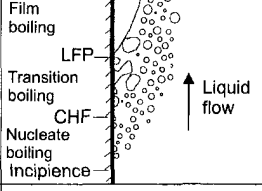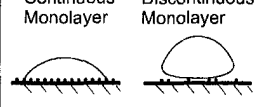
Sakurai et al. (1982) and Groenveld (1982) showed that Berenson's model was only fair in predicting their minimum film boiling temperature data at low pressures and was in extreme error at high pressures.

Metastable Liquid—Homogeneous and Heterogeneous Nucleation Hypotheses. Yao and Henry (1978) and Sakurai et al. (1982) proposed that spontaneous bubble nucleation at the liquid-solid interface is the mechanism for the minimum pool film boiling point. Bubble nucleation can be either heterogeneous, in which the vapor bubbles are produced within cavities at a solid-liquid inter-

Table 2 Summary of the influential LFP parameters

Parameter	Observations/References
Size of liquid mass	• LFP independent of liquid mass size (Gottfried et al. 1966 and Patel and Bell, 1966). • LPF increased with droplet volume (Nishio and Hirata, 1978).
Method of liquid deposition	• LFP differed between steady state drop size technique using a pipet and the transient sessile drop technique (Godleski and Bell, 1966). • LFP increased with droplet velocity (Patel and Bell, 1966, Yao and Cai, 1988; Klinzing et al., 1993; and Labeish, 1994). • LFP did not differ between sessile and impinging drops ($u_o < 5$ m/s) (Bell, 1967 and Nishio and Hirata, 1978).
Liquid subcooling	• Liquid subcooling had little effect on LFP for water on polished aluminum, brass, and stainless steel, but did cause an increased LFP on Pyrex (Baumeister et al. 1970). • Subcooling increased drop lifetime but did not influence the LFP (Hiroyasu et al., 1974). • Subcooling raised the LFP for water and other fluids at high pressures where both sensible and latent heat exchange are significant (Emmerson and Snoek, 1978).
Solid thermal properties	• LFP increases as solid thermal capacitance decreases (Patel and Bell, 1966; Baumeister et al., 1970; and Nishio and Harata, 1978). • Baumeister and Simon (1973) developed a LFP correlation accounts for solid thermal properties. • LFP independent of solid thermal diffusivity (Bell, 1967 and Emmerson, 1975).
Surface conditions	• Gottfried et al. (1966) estimated that the vapor layer beneath a film boiling sessile water drop was on the order of 10 μm, which is on the same length scale as surface aspirates on machine finished surfaces (Bernardin, 1993). Thus, rough surfaces in comparison to polished surfaces would be expected to require a higher LFP to support a thicker vapor layer to avoid liquid-solid contact for a sessile drop (Bradfield 1966). • LFP increased as surface roughness and fouling increased (Baumeister et al., 1970; Baumeister and Simon, 1973; and Nishio and Hirata, 1978). In contrast, Bell (1967) claimed that surface oxide films had a negligible effect on the LFP for droplets. • LFP increased with increasing surface porosity (Avedisian and Koplik, 1987). • LFP decreased with increased advancing contact angle in pool boiling (Kovalev, 1966; Unal et al., 1992; and Labeish, 1994 and Ramilison and Lienhard, 1987).
Pressure	• LFP increased with pressure for various fluids (Nikolayev et al., 1974; Hiroyasu et al., 1974; and Emmerson, 1975; Emmerson and Snoek, 1978) • ($T_{leid} - T_{sat}$) found to remain constant for various pressures (Hiroyasu et al., Emmerson, Nishio and Hirata, 1978, and Testa and Nicotra, 1986). • Rhodes and Bell (1978) observed ($T_{leid} - T_{sat}$) for Freon-114 to be constant over a reduced pressure range of 0.125 to 0.350 and found it to decrease with increasing pressure above this range. Klimenko and Snytin (1990) reported similar findings for four inorganic fluids.

Table 3 Summary of proposed LFP models

Model	Pictorial Description	Relevant Correlations
Hydrodynamic Instability	λ_d	Most dangerous wavelength: $$\lambda_d = 2\pi\left[\frac{3\sigma_f}{g(\rho_f - \rho_g)}\right]^{1/2}$$
Metastable liquid-mechanical stability	P — Isotherm, Saturation curve, Unstable region, Vapor spinodal, Liquid Spinodal — v	Mechanical stabiltiy condition: $$\left(\frac{\partial P}{\partial v}\right)_T = 0$$ Spinodal or liquid superheat limit: (using Van der Waals eqn.) $$T_{thn} = 0.844\, T_c$$
Metastable liquid - kinetic stability	Molecule, No nucleation, Homogeneous nucleation	Homogeneous nucleation limit: $$J = N_f\left(\frac{3\sigma}{\pi m}\right)^{0.5}\exp\left\{\frac{-16\pi\sigma^3}{3k_b T_f\left[\eta P_{sat}(T_f) - P_f\right]^2}\right\}$$ $$\eta = \exp\left\{\frac{v_f\left[P_f - P_{sat}(T_f)\right]}{R T_f}\right\}$$
Thermo-mechanical effect	Film boiling, LFP, Transition boiling, CHF, Nucleate boiling Incipience, Liquid flow	Implicit energy balance for LFP: $$h_g(T_g) - h_f(T_{leid}) = 0.5\left[v_g(T_g) - v_f(T_{leid})\right]$$ $$\left[P_{sat}(T_{leid}) - P_{sat}(T_g)\right]$$
Wettability - contact angle	T_s	Contact angle temperature dependence $$Cos(\theta) = 1 + C\left(T_{ca} - T\right)^{\frac{a}{a-a}}$$
Wettabiltiy - surface adsorption	Continuous Monolayer, Discontinuous Monolayer	Monolayer molecular surface coverage temperature dependence: $$\frac{\Gamma}{\Gamma_o} = \frac{\exp\left(\dfrac{Q_a}{R T_i}\right)}{\left[\dfrac{(2\pi M R T)^{0.5}\Gamma_o}{Na\, P\tau_o}\right] + \exp\left(\dfrac{Q_a}{R T_i}\right)}$$

face as a result of the imperfect wetting of the liquid, or homogeneous, where the bubble nuclei are formed completely within the liquid due to density fluctuations over a duration of 10^{-9} to 10^{-8} s (Skripov et al., 1980).

In the discussion that follows, the metastable state and related physics of homogeneous and heterogeneous nucleation are briefly presented. A more detailed and lengthier discussion of the subject can be found in Skripov (1974) and Carey (1992).

In classical thermodynamics, phase transitions for simple compressible substances are treated as quasi-equilibrium events at conditions corresponding to the saturation state. Between the saturated liquid and saturated vapor states exists a two-phase region where liquid and vapor coexist. Within this region, the temperature and pressure of the two phases must be constant, and the Gibbs function, chemical potential, and fugacity of each phase must be equal. In real-phase transformations, deviations from classical thermodynamics occur under nonequilibrium conditions, such as the superheating of a liquid above its boiling point. These nonequilibrium or metastable states are of practical interest and are important in determining limits or boundaries of real systems.

Shown on the pressure-volume diagram in the pictorial of Table 3 are the superheated liquid and supercooled vapor regions separated by an unstable region. The lines separating these regions are referred to as the liquid and vapor spinodals, which represent the maximum superheating and supercooling limits.

Two different approaches have been used in the literature to predict the superheat limit. The first, based on a mechanical stability condition described by Eberhart and Schnyders (1973) and Carey (1992) for a closed system containing a pure substance which is not in thermodynamic equilibrium, is given as

$$\left(\frac{\partial P}{\partial v}\right)_T < 0. \tag{6}$$

Along the portion of the isotherm between the spinodal lines of Fig. 2, the inequality $\partial p/\partial v > 0$ violates the mechanical stability criterion given by Eq. (6). For this reason, this area is referred to as the unstable region. In the metastable and stable regions, where $\partial p/\partial v < 0$, the liquid or vapor may remain in its form indefinitely. The spinodal limit, at which $\partial p/\partial v = 0$, represents the onset of instability.

Cubic equations of state such as Van der Waals (Spiegler et al., 1963), Himpan (Lienhard and Karimi, 1981), and Berthelot (Blander and Katz, 1975) posses the type of behavior within the vapor dome as discussed above and thus can be used to predict the spinodal limit. Van der Walls equation in terms of the reduced variables $P_r = P/P_c$, $T_r = T/T_c$, and $v_r = v/v_c$, which have been nondimensionalized with the corresponding critical point variables, can be written as
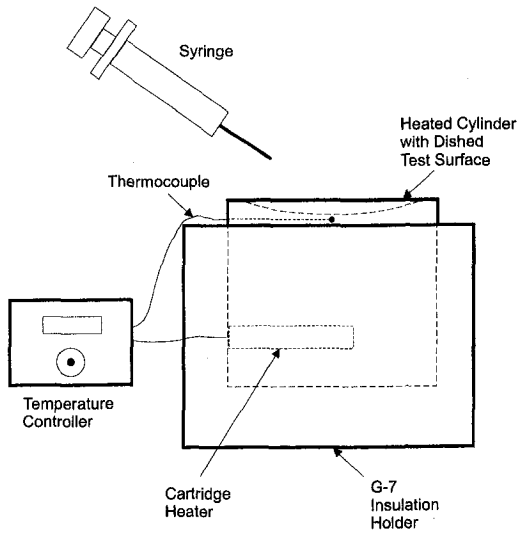
Fig. 2 Schematic diagram of sessile drop experimental apparatus

$$P_r = \frac{8T_r}{3v_r - 1} - \frac{3}{v_r^2}. \tag{7}$$

Using this form of Van der Walls equation of state, the condition of mechanical stability given by Eq. (6), and the fact that $P_r \ll 1$ for most fluids at atmospheric conditions, the thermodynamic homogeneous nucleation temperature limit, T_{thn}, can be derived as (Spiegler et al., 1963)

$$T_{\text{thn}} = 0.844T_c, \tag{8}$$

where absolute temperature quantities are used. Modified forms of Eq. (8) using other equations of state and the success of these models in predicting the superheat limits of liquids are discussed in Carey (1992).

For fluids at higher pressures up to the critical point, Lienhard (1976) offered the following maximum superheat correlation:

$$T_{\text{thn}} = T_c \left[0.905 + 0.095 \left(\frac{T_{\text{sat}}}{T_c} \right)^8 \right], \tag{9}$$

where absolute temperatures are implied.

The second approach to describing the maximum liquid superheat temperature is referred to as the kinetic homogeneous nucleation theory, which bases the temperature and pressure dependence of bubble nucleation on molecular fluctuation probability. At and above saturation conditions, molecular fluctuations occur in such a way to cause a localized decrease in the liquid density, leading to the formation of vapor embryos. The fluctuation probability increases with temperature, and at the superheat temperature limit, the probability of a high bubble embryo formation rate is sufficient to transform the liquid to vapor.

By using conventional bubble nucleation theory, Carey showed how Eq. (10) could be derived to describe the rate of critical-size embryo formation, J, for a superheated liquid

$$J = N_f \left(\frac{3\sigma}{\pi m} \right)^{0.5} \exp \left\{ \frac{-16\pi\sigma^3}{3k_b T_f [\eta P_{\text{sat}}(T_f) - P_f]^2} \right\}, \tag{10}$$

where

$$\eta = \exp \left\{ \frac{v_f [P_f - P_{\text{sat}}(T_f)]}{RT_f} \right\}. \tag{11}$$

Slightly different assumptions have led to minor variations of Eq. (10) by several authors (Skripov, 1974; Blander and Katz, 1975; and Lienhard and Karimi, 1981).

The embryo formation rate given by Eq. (10) increases contin-

uously with temperature. However, because the exponential term has such a strong dependence on the liquid equilibrium temperature, T_f, there exists a small temperature range over which the embryo formation rate begins to increase in a drastic manner. It is within this temperature range that the critical embryo formation rate required to initiate homogeneous nucleation is defined with a corresponding value of T_f equal to the maximum superheat or kinetic homogeneous nucleation temperature. From experimental superheat data for a large variety of fluids at atmospheric pressure, Blander and Katz (1975) obtained a threshold value of 10^{12} m^{-3} s^{-1}. Using this value for J, Eq. (10) can be solved iteratively for the maximum superheat temperature of a given liquid.

Carey (1992) showed how the development of Eq. (10) can be modified to account for the liquid contact angle, θ, and thus describe the heterogeneous nucleation rate of a liquid at a perfectly smooth surface:

$$J = \frac{N_f^{2/3}(1 + \cos\theta)}{2F} \left(\frac{3F\sigma}{\pi m} \right)^{1/2} \exp \left\{ \frac{-16\pi F \sigma^3}{3k_b T_f [\eta P_{\text{sat}}(T_f) - P_f]^2} \right\}, \tag{12}$$

where

$$F = \frac{2 + 3\cos\theta - \cos^3\theta}{4}. \tag{13}$$

The principle factor which is not accounted for in the homogeneous and heterogeneous nucleation models is the influence on the molecular interactions caused by the presence of the solid-liquid interface. Surface energies become influential and continuum fluid theories are not necessarily valid within 50 Å of the interface. Gerwick and Yadigaroglu (1992) recognized that liquid molecular interactions at an interface will be quite different from the bulk liquid. Using statistical mechanics, they developed a modified equation of state for the liquid which was a function of the distance from the solid surface. This equation of state was used to predict the superheat limit of the liquid and thus the rewetting or Leidenfrost temperature of the surface.

Thermomechanical Effect Hypothesis. Schroeder-Richter and Bartsch (1990) refuted the superheated metastable hypothesis of Spiegler et al. (1963) and proposed that the liquid and vapor near the solid surface are in saturated states at different pressures. The authors used a nonequilibrium flow boiling model with conservation equations and appropriate boundary conditions across the liquid-vapor interface, along with assumptions that the liquid immediately in front of the interface is at the Leidenfrost temperature, and that the change in enthalpy during the evaporation is supplied solely by the mechanical energy of the depressurizing liquid to establish the following implicit equation for the Leidenfrost temperature:

$$h_g(T_g) - h_f(T_{\text{leid}})$$
$$= 0.5[v_g(T_g) - v_f(T_{\text{leid}})][P_{\text{sat}}(T_{\text{leid}}) - P_{\text{sat}}(T_g)]. \tag{14}$$

Using saturation tables and an iterative procedure, Eq. (14) can be solved for the LFP.

Wettability Hypotheses. It has been speculated by several researchers that the temperature dependence of the contact angle is influential in controlling the Leidenfrost phenomenon. In a fundamental study by Adamson (1972), a theoretical model was developed that related the molecular surface adsorption of a solid to the liquid-solid contact angle:

$$\cos\theta = 1 + C(T_{co} - T)^{b/(\alpha - b)}, \tag{15}$$

where T_{co} represents a pseudo-critical temperature, or the temperature at which the contact angle goes to zero, C is an integration constant, and b and α are temperature-independent coefficients from a molecular force balance expression given by Adamson. It

is evident from Eq. (15) that the contact angle decreases with increasing temperature, a trend consistent with experimental findings.

Based upon the work of Adamson, Olek et al. (1988) presented a semi-theoretical analysis which suggests that the rewetting temperature or LFP corresponds to a zero contact angle or perfect wetting. The authors suggested that at the temperature, T_{co}, where the contact angle goes to zero, the liquid drop spreads into a sufficiently thin film such that enough vapor can be generated to disjoin the film from the surface. Olek et al. were only able to provide experimental data for two water-nonmetallic solid systems with which to evaluate their model. Their comparison showed fair agreement between the predicted and measured temperature-dependent contact angle trends. However, they failed to provide Leidenfrost temperature data for the two surfaces.

Segev and Bankoff (1980) offered a more plausible explanation of the Leidenfrost phenomenon based on wetting characteristics. They proposed that wetting of a hot solid surface by a liquid is controlled by a microscopic precursor film which advances in front of the much thicker spreading liquid film. The presence of the thin film, which is required for the advancing and wetting of the remainder of the liquid, is controlled by the temperature-dependent surface adsorption characteristics. The precursor film thickness decreases with increasing temperature and drops off sharply as the temperature threshold (the LFP) is reached. Above this temperature, adsorption of the liquid molecules beyond a monolayer is no longer possible, and surface wetting cannot occur.

Segev and Bankoff based their model on the Langmuir adsorption isotherm

$$\frac{\Gamma}{\Gamma_o} = \frac{\exp\left(\dfrac{Q_a}{RT_i}\right)}{\left(\dfrac{(2\pi MRT)^{0.5}\Gamma_o}{N_a P \tau_o}\right) + \exp\left(\dfrac{Q_a}{RT_i}\right)} \tag{16}$$

which describes the fraction of total monolayer surface adsorption sites, Γ_o, occupied by foreign molecules in terms of the liquid-solid interface temperature, T_i, heat of adsorption, Q_a, and residence time of a molecule in the adsorbed state, τ_o. Segev and Bankoff claimed that the LFP corresponds to a surface monolayer coverage fraction of 0.9, and by using $\Gamma_o = 10^{19}$ molecules/m^2 and $\tau_o = 10^{-13}$ s, Eq. (16) can be solved explicitly for the surface temperature if the heat of adsorption of the fluid's vapor on the solid is known.

3 Experimental Apparatus and Procedure

The sessile drop apparatus shown in Fig. 2 was used to study the evaporation characteristics of droplets on a heated surface. In particular, the liquid/solid interface temperature corresponding to the Leidenfrost point was determined from droplet evaporation curves for a variety of operating conditions. The sessile drop facility consisted of an instrumented test heater module, temperature controller, and a syringe. The various working fluids included acetone, benzene, FC-72, an inert fluorocarbon produced by the 3M corporation, and distilled water. Several test heater modules were fabricated from either a solid aluminum or copper cylinder with a shallow concave surface designed to contain the liquid droplets during states of transition and film boiling. To investigate surface material effects on the LFP, several copper heater modules were also electroplated with either silver or nickel to a thickness of 0.025 mm. The heater module was mounted in an insulating shell formed from G-7 phenolic, which is capable of withstanding surface temperatures of 300°C for short durations. An Ogden Type 33 temperature controller, a Watlow 150 Watt cartridge heater, and a calibrated Chromel-Alumel (type K) thermocouple (calibrated accuracy = ±0.2°C) located 2.5 mm beneath the center of the test surface were used to monitor and control the surface temperature. A finite element analysis and several thermocouple measurements near the edge of the module were used to verify that the temperature distribution across the plane just beneath the surface was uniform and representative of the surface temperature. Three different surface finishes including polished, particle blasted, and rough sanded, with arithmetic average surface roughness values of 97, 970, and 2960 nm, respectively, were used in the study. A glass syringe with a 24-gauge hypodermic needle having a 0.58-mm (0.023-in.) outer diameter, was used to slowly dispense droplets of uniform diameter onto the test heater. A static force balance between gravity and surface tension dictated the nearly consistent droplet diameter for a given fluid. A high-speed Ektapro motion analyzer was used to verify that the slow droplet generation technique produced uniformly sized droplets within an error band of ten percent. Preliminary tests, performed with water and different diameter needles, revealed no dependence of the LFP on initial droplet size. This is consistent with findings reported by Gaottfried et al. (1966) and Patel and Bell (1966). Consequently, only one initial droplet diameter (fluid dependent) was used in this study.

For each test, single droplet evaporation times were recorded versus surface temperature over a temperature range encompassing the entire boiling spectrum for each particular fluid. The experiments began by dispensing a single drop from a syringe onto the center of the test surface at a temperature well within the film boiling regime from an approximate height of 1 cm. A manual digital stopwatch was used to record the time to the nearest tenth of a second for complete visual evaporation of the drop. To minimize timer (±0.1 s) and initial droplet size (±10 percent) errors, five evaporation times were recorded for each temperature increment and then averaged together. This procedure was performed for ten-degree centigrade surface temperature increments from a temperature within the fluid's film boiling regime down to the boiling incipience temperature, with finer two degree centigrade increments being made around the LFP. Each set of droplet evaporation data was used to generate a droplet evaporation curve, similar to the one displayed in Fig. 1(b), from which the LFP was identified by interpolation. The Leidenfrost temperature, or droplet/solid interface temperature corresponding to the LFP, was then determined with Eq. (3), using the measured surface temperature corresponding to the LFP.

The sources of experimental error in determining the Leidenfrost temperature included uncertainties in initial droplet size (±10 percent), droplet evaporation time (±0.1 s), and surface temperature measurement (±0.2°C). An additional error was imposed by the graphical LFP interpolation uncertainty caused by the 2°C gap between data points near the LFP on the droplet evaporation plots. The uncertainty in droplet evaporation time was deemed minimal since the accuracy of the timer was nearly two orders of magnitude smaller than typical droplet evaporation times near the LFP. The uncertainty in droplet size was minimized by taking the average evaporation time of five droplets at each data point. The temperature measurement uncertainty combined with the graphical LFP interpolation error created by the 2°C gap between data points, resulted in a total experimental uncertainty of 4.4°C. This was found to be consistent with reproducibility tests that revealed the LFP measurements were repeatable within ±5°C.

An extensive database was required for identifying key influential parameters and to assess several analytical and theoretical models. Consequently, the experimental procedure was performed for four different test fluids with and without degassing, various degrees of liquid subcooling, four different surface materials, a variety of surface finishes, and different forms of surface contamination. To investigate the effect of surface impurities left behind from previous drops, two different tests were performed. In one case, the surface was wiped clean with a fine tissue between successive drops, and in the other case, the surface was left as is. More detailed operating conditions for the various tests are discussed with the experimental results.

Table 4 Leidenfrost temperatures for various fluids and aluminum surface conditions

Fluid	T_{leid} (°C) Surface Finish		
	Polished	Particle Blasted	Rough Sanded
Acetone (wiped)	135 [130, 140, 135]	155 [160, 150]	160 [160, 160]
Acetone (unwiped)	185 [185, 185]	200 [195, 205]	178 [180, 175]
Benzene (wiped)	175	220	218
Benzene (unwiped)	180	215	215
FC-72 (wiped)	90	110	120
FC-72 (unwiped)	115	110	120
Water (wiped)	171 [175, 180, 160, 170]	250 [250, 250]	263 [260, 265]
Water (unwiped)	225 [220, 230]	280 [280, 280]	263 [260, 265]

4 Experimental Results and Discussion

In the discussions that follow, the reported empirical Leidenfrost temperatures correspond to measured surface temperatures at the LFP. However, in the evaluations of the LFP models (Table 6), both the empirical Leidenfrost temperatures and adjusted LFP values (using Eq. (3) to account for the liquid/solid interface) are presented.

Table 4 presents the LFP data for acetone, benzene, FC-72, and distilled water on three different aluminum surface finishes for both wiped and unwiped conditions between successive drops. The average LFP values are displayed with large text in Table 4 while the small test in brackets indicates Leidenfrost temperatures from individual runs when more than one test was performed for a single set of operating conditions. The focus of this experimental data was to study the effects of fluid properties, surface roughness, and surface contamination on the LFP.

The Leidenfrost temperature data of Table 4 indicate the following general trends:

Effect of Surface Roughness: For all test fluids, polished surfaces had significantly lower Leidenfrost temperatures than particle blasted and rough sanded surfaces. The surface roughness dependence of the Leidenfrost temperature is speculated to be related to intermittent liquid-solid contact caused by surface aspirates poking through the thin vapor layer, which, as reported by Labeish (1994), is on the order of 1 μm. As the surface roughness increases, a thicker vapor layer, and hence a higher surface temperature, is required to keep the liquid separated from the solid surface. This effect would be expected to taper off as surface roughness increases, which is observed in the similar Leidenfrost temperatures for the particle blasted and rough sanded surfaces.

Effect of Surface Contamination: A wiped surface generally had a considerably lower Leidenfrost temperature than an unwiped surface. This was most evident for the polished surface and to a lesser degree for the particle blasted and rough sanded surfaces.

The surface deposits left from previous drops tended to serve as vapor bubble nucleation sources when making contact with newly deposited drops, much in the same way as the surface aspirates acted on the rougher surfaces. With deposits present, a higher surface temperature was required to sustain film boiling. This finding is consistent with those of Baumeister et al. (1970) who found that the Leidenfrost temperature for water on a freshly polished aluminum surface was 155°C, 70°C less than that of a conventional contaminated surface. It is intuitively obvious that surface contamination from previous drops will act to increase the roughness on a polished surface to a much larger degree than for an initially much rougher surface. This explains why the Leidenfrost temperature for a polished surface is highly influenced by deposits while the rougher surfaces are not.

Table 5 presents Leidenfrost temperature data for water and a variety of polished surface materials. The numbers in large text indicate average LFP temperature values while the numbers in small text and brackets indicate single experimental data points. The accuracy and sensitivity of the measurements resulted in a ±15°C band around the average Leidenfrost temperatures tabulated herein. The focus of this portion of the study was to investigate the influences of surface material, surface contamination from polishing pastes, surface roughness on the polished level, liquid subcooling, and liquid degassing on the LFP.

Effect of Surface Material and Polishing Paste Residue: Leidenfrost temperature values were obtained for water on polished aluminum, silver, nickel, and copper. The average Leidenfrost temperature is nearly identical for the aluminum, silver, and nickel surfaces but is significantly higher for the copper surface. The higher LFP value of the copper surface is speculated to be the result of surface roughening which accompanied large amounts of surface oxidation during heating. Jeschar et al. (1984) also reported a higher Leidenfrost temperature for copper compared to nickel and, as in this study, attributed this to roughening of the copper test piece by heavy oxidation. Labeish (1994) reported

Table 5 Measured Leidenfrost temperatures for water on polished surfaces

Surface	T_{leid} (°C)	Notes
Aluminum	$170 \begin{bmatrix} 170 \\ 170 \end{bmatrix}$	• Study: material effect • Surface: polished with 45, 30, 15, 9, 6, & 3 micron diamond paste and chemically cleaned
Silver	$176 \begin{bmatrix} 185 & 170 \\ 190 & 160 \end{bmatrix}$	• Study: material effect • Surface: polished with 45, 30, 15, 9, 6, & 3 micron diamond paste, silver plated, polished with Simichrome, wiped with acetone, oxidized upon heating
Nickel	$173 \begin{bmatrix} 175 \\ 170 \end{bmatrix}$	• Study: material effect • Surface: polished with 45, 30, 15, 9, 6, & 3 micron diamond paste, nickel plated, wiped with acetone, no apparent oxidation
Copper	$198 \begin{bmatrix} 185 & 200 \\ 210 & \end{bmatrix}$	• Study: material effect • Surface: polished with 45, 30, 15, 9, 6, & 3 micron diamond paste and chemically cleaned, heavy oxidation upon heating surface
Nickel	$181 \begin{bmatrix} 180 & 190 \\ 175 & 190 \\ 170 & \end{bmatrix}$	• Study: material effect • Surface: polished with Simichrome, nickel plated, wiped with acetone, no apparent oxidation
Copper	$193 \begin{bmatrix} 195 \\ 190 \end{bmatrix}$	• Study: material effect • Surface: polished with Simichrome paste, heavy oxiation upon heating surface
Aluminum	$175 \begin{bmatrix} 170 & 175 \\ 180 & \end{bmatrix}$	• Study: roughness effect • Surface Prep.: polished with 45 micron paste
Aluminum	$181 \begin{bmatrix} 190 & 180 \\ 190 & 165 \end{bmatrix}$	• Study: roughness effect • Surface: polished with 45, 30, & 15 micron diamond paste
Aluminum	$185 \begin{bmatrix} 180 \\ 190 \end{bmatrix}$	• Study: roughness effect • Surface: polished with 45, 30, 15, 9, 6, & 3 micron diamond paste
Aluminum	$171 \begin{bmatrix} 175 & 160 \\ 180 & 170 \end{bmatrix}$	• Study: roughness effect • Surface: polished w/ 45, 30, 15, 9, 6, & 3 micron diamond paste then with Simichrome paste
Aluminum	$178 \begin{bmatrix} 190 \\ 165 \end{bmatrix}$	• Study: degassing effects (water degassed) • Surface: polished with 9, 6, & 3 micron diamond paste and chemically cleaned
Aluminum	175	• Study: subcooling effect (T_f = 90 °C) • Surface: polished with 45, 30, 15, 9, 6, & 3 micron diamond paste and chemically cleaned
Aluminum	170	• Study: subcooling effect (T_f = 60 °C) • Surface: polished with 45, 30, 15, 9, 6, & 3 micron diamond paste and chemically cleaned
Aluminum	160	• Study: polishing paste effect • Surface: polished with Simichrome, then soaked & wiped with acetone

samples with the following surface finish preparations: polished with Simichrome paste; polished with Simichrome paste followed by soaking and wiping with acetone to remove the paste residue; and, polished with an array of diamond compounds followed by an acid bath chemical cleaning. The lack of variability in the LFP values for these three surfaces suggests that the polishing paste residue has little influence on the LFP.

Effect of Surface Roughness on the Polished Level: Average Leidenfrost temperatures for water on aluminum surfaces polished with different grades of diamond polishing compound all fell within a 15°C band, thus indicating no significant dependence of the LFP on surface roughness on the polished level.

Effect of Liquid Subcooling: For identical surface conditions, water liquid subcoolings of 10, 40, and 80°C resulted in Leidenfrost temperatures of 170, 170, and 175°C, respectively. The lack of sensitivity of the LFP on liquid subcooling results because the small amount of liquid contained in a single droplet, regardless of initial temperature, is rapidly heated to near saturated conditions when placed on the surface. This finding was also reported by Hiroyasu et al. (1974) and Grissom and Wierum (1981).

Effect of Liquid Degassing: Table 5 lists average Leidenfrost temperatures of 170°C and 178°C for nondegassed and degassed water, respectively, on a polished aluminum surface. Negligible differences of less than five percent were observed between nondegassed and degassed Leidenfrost temperatures for acetone and FC-72 on polished aluminum as well. Clearly, the effect of air and other non-condensible gases within the liquid on the LFP is minimal.

5 Assessment of Models

As mentioned previously, the temperature generally measured and reported as the LFP corresponds to that of the solid in the near vicinity of the surface. However, boiling is an interfacial phenomenon, and thus it is better practice to associate the LFP with the temperature of the liquid-solid interface. In the model assessments that follow, both the empirical Leidenfrost temperatures measured within the solid, and adjusted LFP values (using Eq. (3) to account for the liquid/solid interface) are presented in Table 6 for comparison.

Evaluation of Instability Models. To investigate whether or not a Taylor-type instability could control the Leidenfrost phenomenon, a length scale comparison can be made between the droplet diameter and the Taylor most dangerous interfacial wavelength, λ_d. For Benzene, FC-72, and water the corresponding values of λ_d are 17.7, 8.4, and 27.3 mm, respectively. These wavelengths are of the same order or larger than typical droplet diameters, which indicates that the Taylor interfacial instability, while possibly suitable for pool boiling analysis, does not lend itself to isolated

theoretical rewetting wall temperatures for smooth surfaces of different materials wetted by water drops. Accounting for surface thermal properties and neglecting surface effects, nearly identical rewetting temperatures of 270, 282, and 292°C were predicted for copper, nickel, and carbon steel, respectively. These predictions, while higher in absolute value than those reported in this study, indicate a relative insensitivity of the LFP to surface chemistry effects.

As the data of Table 5 indicates, no significant difference was observed in the Leidenfrost temperatures of polished aluminum

Table 6 Comparison of various Leidenfrost temperature (°C) models to experimental data for a polished aluminum surface

Fluid	Measured Leidenfrost temperature (°C)	Corrected liquid/solid interface Leidenfrost temperature (eqn. (3))	Berenson (1961) hydro-dynamic model	Thermo-dynamic homogen. nucleation limit temperature	Kinetic homogen. nucleation limit temperature	Baumeister and Simon (1973) correlation	Schroeder-Richter and Bartsch (1990) thermo-mechanical model
Acetone	134	132	152	156	198	130	‡
Benzene	175	172	140	201	239	171	180
Water	170	162	152	273	310	156	221
FC-72	90	89	‡	106	144	102	116

‡ Fluid properties unavailable to evaluate model.

boiling drops. Table 6 compares predictions for T_{leid}, using Berenson's (1961) model for T_{mfb} (Eq. (5)) to experimentally measured sessile drop Leidenfrost temperatures for several of the fluids used in this study. The predictions show significant error for acetone and benzene and give only satisfactory results for water.

Evaluation of Metastable Liquid Models. Two theoretical models, the thermodynamic or mechanical stability model and the kinetic homogeneous nucleation model, have been developed using entirely different approaches to predict the maximum superheat temperature of liquids. However, attempting to use these models to predict the Leidenfrost temperature for sessile drops has not met reasonable success.

The Leidenfrost point correlation of Baumeister and Simon (1973) contains two sources of concern. First, in developing a conduction model to account for a decrease in the surface temperature at liquid-solid contact, the authors fail to explain how they arrived at the chosen value of an average heat transfer coefficient. Second and most importantly, Baumeister and Simon introduce a surface energy correction factor to the superheat model of Spiegler et al. While this factor leads to a correlation which successfully fits the data, the results may be deceiving in that they suggests that homogeneous nucleation, around which the correlation is constructed, is the mechanism governing the Leidenfrost phenomenon, when in fact, it may not be.

Experimental Leidenfrost temperatures for various liquids on a polished aluminum surface from the current study are compared to thermodynamic and kinetic superheat limits as well as the correlation of Baumeister and Simon (1973) in Table 6. All predictions were made with absolute temperature quantities and then converted to degrees Celsius. For the theoretical metastable liquid models, the superheat limits are considerably higher than the measured Leidenfrost temperatures for all fluids tested, consistent with the results of Spiegler et al. (1963). The semi-empirical correlation by Baumeister and Simon agrees quite well with the experimental data of the present study, but as previously mentioned, it fails to accurately model the physics governing the process. Obviously, superheat criteria alone do not accurately describe the Leidenfrost phenomenon for sessile drops on a heated surface.

While elegant, the modified equation of state and homogeneous nucleation model of Gerwick and Yadigaroglu (1992) involved several assumptions which severely limit its applicability and accuracy. First, a simple hard-sphere potential interaction model using London dispersion forces was used to describe the molecular interactions. This limits the model's applicability to nonpolar liquids, since liquids such as water, with highly polar hydrogen bonding forces, would not lend themselves to such modeling with any high degree of accuracy. Second, a parameter describing the strength of the wall-fluid interactions was stated to be unknown for most practical applications. Consequently, a simplified model which related this parameter to the contact angle was employed. The major argument against this simplification is that the contact angle is typically measured over a distance which is at least six orders of magnitude larger than the thickness of the fluid layer influenced by the presence of the solid surface. In fact, Adamson (1982) has hypothesized that the microscopic contact angle at the leading edge of the liquid film, which is on the order of several molecular diameters in thickness, is significantly smaller than the macroscopic contact angle commonly reported. In addition, the contact angle is highly influenced by surface roughness and impurities (Miller and Neogi, 1985; Bernardin et al., 1997), making it a highly undefined variable.

Evaluation of Nonequilibrium Model. Table 6 compares Leidenfrost temperatures predicted by Eq. (14) to experimentally measured values for several different fluids. The prediction for Benzene is quite good, while that for FC-72 is satisfactory, and the estimate for water is extremely poor.

Several problems exist in the development of Eq. (14) and its application to predicting the Leidenfrost temperature for droplets. First, the original model was constructed to emulate a vertical dry-out flow boiling situation, a condition far from that of a sessile or impinging droplet. Next, and more importantly, the concept of saturated states at different pressures for the liquid and vapor rather than metastable superheating of the liquid at constant pressure is unsupported. Metastable states for fluids have been frequently observed (Avedisian, 1982; Shepherd and Sturtevant, 1982; McCann et al., 1989) and the physics of such nonequilibrium states have been well documented (Eberhart and Schnyders, 1973; Skripov, 1974; Lienhard and Karimi, 1978; Carey, 1992). In fact, liquid superheating forms the entire well established basis for bubble nucleation theory in boiling (Han and Griffith, 1965; Blander et al., 1971).

Evaluation of Wettability Models. The reasoning behind the contact angle model of Olek et al. (1988) appears unrealistic. In addition, the implicit equation for the LFP is difficult to verify since the required coefficients are only available for a few liquid-solid systems for which no Leidenfrost temperature data exists. The temperature-dependent contact angle measurements found by Bernardin and Mudawar (1997) for water on aluminum show little indication of a zero contact angle condition acting as the Leidenfrost point mechanism. Also in contrast to the model of Olek et al., nearly identical Leidenfrost temperatures were obtained in this study for two identically polished aluminum surfaces, one of which was left with a polishing paste residue, and the other which was chemically cleaned. Also, nearly identical Leidenfrost temperatures were obtained for aluminum, silver, and nickel surfaces, all of which have different wetting characteristics. The contact angle depends to such a large extent on the surface conditions (roughness, contamination, adsorption), as well as on liquid velocity and direction, it is a difficult parameter to characterize and effectively utilize. Thus it can be concluded that while surface wetting, as measured by the contact angle, may play a role in boiling heat transfer, it is not the controlling LFP mechanism.

The surface adsorption hypothesis of Segev and Bankoff (1980) is very difficult to verify for a liquid-surface combination because it requires the corresponding heat of adsorption of the fluid's vapor on the solid surface. Correct knowledge of the chemical makeup of a solid surface is very difficult to obtain. The presence of oxide layers or adsorbed layers of grease and other impurities changes the surface chemistry considerably. In addition, the experimental data of this study tends to disprove the hypothesis proposed by Segev and Bankoff. Using heat of adsorption for water vapor on aluminum oxide (McCormick and Westwater, 1965) and nickel oxide (Matsuda et al., 1992), Eq. (16) predicts Leidenfrost temperatures of 162 and 425°C for saturated water on aluminum and nickel, respectively. The predicted LFP value for the aluminum surface agrees reasonably well with the corresponding experimental value of 170°C, however, the model fails miserably for the nickel surface which had an experimental Leidenfrost temperature of 175°C. Segev and Bankoff's model suggests that the LFP for an aluminum surface possessing a polishing paste residue would be significantly different from an identically polished surface without the residue, a trend not observed in the experimental data of this study.

6 Conclusions

Sessile drop evaporation experiments were performed for a wide variety of operating conditions to establish a large LFP data base for identifying key influential parameters and assessing existing LFP models. From the experimental results, several key conclusions concerning the influential LFP parameters can be drawn.

- Liquid subcooling, the presence of dissolved gasses, and surface roughness on the polished level do not significantly influence the Leidenfrost temperature.
- Surface thermal properties will act to control the interface and hence Leidenfrost temperature. However, aside from thermal properties, the LFP is relatively insensitive to surface material as far as surface energies and wetting characteristics are concerned.
- Surface roughness, beyond that on the polished level, appears to

be a dominant parameter in controlling the Leidenfrost behavior. The data indicate, that for a given fluid, a polished surface possesses a relatively low Leidenfrost temperature in comparison to a particle blasted or rough sanded surface. In addition, surface impurities or deposits act to increase the relative surface roughness and the corresponding Leidenfrost temperature.

Sound arguments supported by experimental data were used to assess several hypothetical models of the LFP mechanism. These models were shown to lack robustness and were ineffective in predicting the Leidenfrost temperature. A model which successfully captures the Leidenfrost mechanism is currently being developed to account for several parameters which were found to actively influence the LFP in both previous investigations and the current study. These parameters include thermal properties of the solid, thermal and thermodynamic properties of the liquid, solid surface structure, pressure, and droplet impact velocity.

References

Adamson, A. W., 1972, "Potential Distortion Model for Contact Angle and Spreading II. Temperature Dependent Effects," *J. Colloid Interface Sci.,* Vol. 44, pp. 273–281.

Adamson, A. W., 1982, *Physical Chemistry of Surfaces,* John Wiley and Sons, Inc., New York.

Avedisian, C. T., 1982, "Effect of Pressure on Bubble Growth Within Liquid Droplets at the Superheat Limit," ASME JOURNAL OF HEAT TRANSFER, Vol. 104, pp. 750–757.

Avedisian, C. T., and Koplik, J., 1987, "Leidenfrost Boiling of Methanol Droplets on Hot Porous Ceramic Surfaces," *Int. J. Heat Mass Transfer,* Vol. 30, pp. 379–393.

Baumeister, K. J., Henry, R. E., and Simon, F. F., 1970, "Role of the Surface in the Measurement of the Leidenfrost Temperature," *Augmentation of Convective Heat and Mass Transfer,* A. E. Bergles and R. L. Webb, eds., ASME, New York, pp. 91–101.

Baumeister, K. J., and Simon, F. F., 1973, "Leidenfrost Temperature—Its Correlation for Liquid Metals, Cryogens, Hydrocarbons, and Water," ASME JOURNAL OF HEAT TRANSFER, Vol. 95, pp. 166–173.

Bell, K. J., 1967, "The Leidenfrost Phenomenon: A Survey," *Chem. Eng. Prog. Symposium Series,* Vol. 63, AIChE, New York, pp. 73–82.

Berenson, P. J., 1961, "Film Boiling Heat Transfer from a Horizontal Surface," ASME JOURNAL OF HEAT TRANSFER, Vol. 83, pp. 351–358.

Bernardin, J. D., 1993, Intelligent Heat Treatment of Aluminum Alloys: Material, Surface Roughness, and Droplet-Surface Interaction Characteristics, Masters thesis, Purdue University, West Lafayette, Indiana. IN.

Bernardin, J. D., and Mudawar, I., 1995, "Validation of the Quench Factor Technique in Predicting Hardness in Heat Treatable Aluminum Alloys," *Int. J. Heat Mass Transfer,* Vol. 38, pp. 863–873.

Bernardin, J. D., Mudawar, I., and Franses, E. I., 1997, "Contact Angle Temperature Dependence for Water Droplets on Practical Aluminum Surfaces," *Int. J. Heat Mass Transfer,* Vol. 40, pp. 1017–1033.

Blander, M., Hengstenberg, D., and Katz, J. L., 1971, "Bubble Nucleation in *n*-Pentane, *n*-Hexane, *n*-Hentane + Hexadecane Mixtures, and Water," *J. Phys. Chem.,* Vol. 75, pp. 3613–3619.

Blander, M., and Katz, J. L., 1975, "Bubble Nucleation in Liquids," *Amer. Inst. Chem. Eng. J.,* Vol. 21, pp. 833–848.

Blaszkowska-Zakrzewska, H., 1930, "Rate of Evaporation of Liquids from a Heated Metallic Surface," *Bulletin International de l'Academie Polonaise,* Vol. 4a–5a, pp. 188–190.

Bradfield, W. S., 1966, "Liquid-Solid Contact in Stable Film Boiling," *I & E C Fundamentals,* Vol. 5, pp. 200–204.

Carey, V. P., 1992, *Liquid-Vapor Phase Change Phenomena: An Introduction to the Thermophysics of Vaporization and Condensation Processes in Heat Transfer Equipment,* Hemisphere, New York.

Eberhart, J. G., and Schnyders, H. C., 1973, "Application of the Mechanical Stability Condition to the Prediction of the Limit of Superheat for Normal Alkanes, Ether, and Water," *J. Phys. Chem.,* Vol. 77, pp. 2730–2736.

Eckert, E. R. G., and Drake, Jr., R. M., 1972, *Analysis of Heat and Mass Transfer,* McGraw-Hill, New York.

Emmerson, G. S., 1975, "The Effect of Pressure and Surface Material on the Leidenfrost Point of Discrete Drops of Water," *Int. J. Heat Mass Transfer,* Vol. 18, pp. 381–386.

Emmerson, G. S., and Snoek, C. W., 1978, "The Effect of Pressure on the Leidenfrost Point of Discrete Drops of Water and Freon on a Brass Surface," *Int. J. Heat Mass Transfer,* Vol. 21, pp. 1081–1086.

Gerweck, V., and Yadigaroglu, G., 1992, "A Local Equation of State for a Fluid in the Presence of a Wall and its Application to Rewetting," *Int. J. Heat Mass Transfer,* Vol. 35, pp. 1823–1832.

Godleski, E. S., and Bell, K. J., 1966, "The Leidenfrost Phenomenon for Binary Liquid Solutions," *Third International Heat Transfer Conference,* Vol. 4, Chicago, IL, AIChE, New York, pp. 51–58.

Gottfried, B. S., Lee, C. J., and Bell, K. J., 1966, "The Leidenfrost Phenomenon: Film Boiling of Liquid Droplets on a Flat Plate," *Int. J. Heat Mass Transfer,* Vol. 9, pp. 1167–1187.

Grissom, W. M., and Wierum, F. A., 1981, "Liquid Spray Cooling of a Heated Surface," *Int. J. Heat Mass Transfer,* Vol. 24, pp. 261–271.

Han, C. Y., and Griffith, P., 1965, "The Mechanism of Heat Transfer in Nucleate Pool Boiling—Part I," *Int. J. Heat Mass Transfer,* Vol. 8, pp. 887–904.

Hiroyasu, H., Kadota, T., and Senda, T., 1974, "Droplet Evaporation on a Hot Surface in Pressurized and Heated Ambient Gas," *Bulletin of the JSME,* Vol. 17, pp. 1081–1087.

Hosler, E. R., and Westwater, J. W., 1962, "Film Boiling on a Horizontal Plate," *ARS J.,* Vol. 32, pp. 553–558.

Jeschar, R., Scholz, R., and Reiners, U., 1984, "Warmeubergang bei der zweiphasigen spritzwasserkuhlung," *Gas-Warme Int.,* Vol. 33, p. 6.

Klimenko, V. V., and Snytin, S. Y., 1990, "Film Boiling Crisis on a Submerged Heating Surface," *Exp. Thermal Fluid Sci.,* Vol. 3, pp. 467–479.

Klinzing, W. P., Rozzi, J. C., and Mudawar, I., 1992, "Film and Transition Boiling Correlations for Quenching of Hot Surfaces with Water Sprays," *J. Heat Treating,* Vol. 9, pp. 91–103.

Kovalev, S. A., 1966, "An Investigation of Minimum Heat Fluxes in Pool Boiling of Water," *Int. J. Heat Mass Transfer,* Vol. 9, pp. 1219–1226.

Labeish, V. G., 1994, "Thermohydrodynamic Study of a Drop Impact Against a Heated Surface," *Exp. Thermal Fluid Sci.,* Vol. 8, pp. 181–194.

Lienhard, J. H., 1976, "Correlation for the Limiting Liquid Superheat," *Chem. Eng. Sci.,* Vol. 31, pp. 847–849.

Lienhard, J. H., and Karimi, A. H., 1978, "Corresponding States Correlations of the Extreme Liquid Superheat and Vapor Subcooling," ASME JOURNAL OF HEAT TRANSFER, Vol. 100, pp. 492–495.

Matsuda, T., Taguchi, H., and Nagao, M., 1992, "Energetic Properties of NiO Surface Examined by Heat-of-Adsorption Measurement," *J. Thermal Analysis,* Vol. 38, pp. 1835–1845.

McCann, H., Clarke, L. J., and Masters, A. P., 1989, "An Experimental Study of Vapor Growth at the Superheat Limit Temperature," *Int. J. Heat Mass Transfer,* Vol. 32, pp. 1077–1093.

McCormick, J. L., and Westwater, J. W., 1965, "Nucleation Sites for Dropwise Condensation," *Chem. Eng. Sci.,* Vol. 20, pp. 1021–1036.

Miller, C. A., and Neogi, P., 1985, *Interfacial Phenomena,* Marcel Dekker, New York.

Nikolayev, G. P., Bychenkov, V. V., and Skripov, V. P., 1974, "Saturated Heat Transfer to Evaporating Droplets from a Hot Wall at Different Pressures," *Heat Transfer—Soviet Research,* Vol. 6, pp. 128–132.

Nishio, S., and Hirata, M., 1978, "Direct Contact Phenomenon between a Liquid Droplet and High Temperature Solid Surface," *Sixth International Heat Transfer Conference,* Vol. 1, Toronto, Canada, Hemisphere, New York, pp. 245–250.

Olek, S., Zvirin, Y., and Elias, E., 1988, "The Relation between the Rewetting Temperature and the Liquid-Solid Contact Angle," *Int. J. Heat Mass Transfer,* Vol. 31, pp. 898–902.

Patel, B. M., and Bell, K. J., 1966, "The Leidenfrost Phenomenon for Extended Liquid Masses," *Chem. Eng. Progress Symposium Series,* Vol. 62, pp. 62–71.

Ramilison, J. M., and Lienhard, J. H., 1987, "Transition Boiling Heat Transfer and the Film Transition Regime," ASME JOURNAL OF HEAT TRANSFER, Vol. 109, pp. 746–752.

Rhodes, T. R., and Bell, K. J., 1978, "The Leidenfrost Phenomenon at Pressures up to the Critical," *Sixth International Heat Transfer Conference,* Vol. 1, Toronto, Canada, Hemisphere, New York, pp. 251–255.

Sakurai, A., Shiotsu, M., and Hata, K., 1982, "Steady and Unsteady Film Boiling Heat Transfer at Subatmospheric and Elevated Pressures," *Heat Transfer in Nuclear Reactor Safety,* S. G. Bankoff and N. H. Afgan eds., Hemisphere New York, pp. 301–312.

Schroeder-Richter, D., and Bartsch, G., 1990, "The Leidenfrost Phenomenon caused by a Thermo-Mechanical effect of Transition Boiling: A Revisited Problem of Non-Equilibrium Thermodynamics," *Fundamentals of Phase Change: Boiling and Condensation,* ASME, New York, pp. 13–20.

Segev, A., and Bankoff, S. G., 1980, "The Role of Adsorption in Determining the Minimum Film Boiling Temperature," *Int. J. Heat Mass Transfer,* Vol. 23, pp. 637–642.

Shepherd, J. E., and Sturtevant, B., 1982, "Rapid Evaporation at the Superheat Limit," *J. Fluid Mechanics,* Vol. 121, pp. 379–402.

Skripov, V. P., 1974, *Metastable Liquids,* John Wiley and Sons, New York.

Skripov, V. P., Sinitsyn, E. N., and Pavlov, P. A., 1980, *Thermal and Physical Properties of Liquids in the Metastable State,* Atomizdat, Moscow.

Spiegler, P., Hopenfeld, J., Silberberg, M., Bumpus, Jr., C. F., and Norman, A., 1963, "Onset of Stable Film Boiling and the Foam Limit," *Int. J. Heat Mass Transfer,* Vol. 6, pp. 987–994.

Taylor, G. I., 1950, "The Instability of Liquid Surfaces when Accelerated in a Direction Perpendicular to their Plane, I," *Proc. Royal Society of London,* Vol. A201, p. 192.

Testa, P., and Nicotra, L., 1986, "Influence of Pressure on the Leidenfrost Temperature and on Extracted Heat Fluxes in the Transient Mode and Low Pressure, *Transactions of the ASME,* Vol. 108, pp. 916–921.

Unal, C., Daw, V., and Nelson, R. A., 1992, "Unifying the Controlling Mechanisms for the Critical Heat Flux and Quenching: The Ability of Liquid to Contact the Hot Surface," ASME JOURNAL OF HEAT TRANSFER, Vol. 114, pp. 972–982.

Xiong, T. Y., and Yeun, M. C., 1990, "Evaporation of a Liquid Droplet on a Hot Plate," *Int. J. Heat Mass Trans.,* Vol. 34, pp. 1881–1894.

Yao, S. C., and Henry, R. E., 1978, "An Investigation of the Minimum Film Boiling Temperature on Horizontal Surfaces," *Transactions of the ASME,* Vol. 100, pp. 263–266.

Yao, S. C., and Cai, K. Y., 1988, "The Dynamics and Leidenfrost Temperature of Drops Impacting on a Hot Surface at Small Angles," *Exp. Thermal Fluid Sci.,* Vol. 1, pp. 363–371.

Zuber, N., 1958, "On the Stability of Boiling Heat Transfer," *Transactions of the ASME,* pp. 711–720.

52

Rate of evaporation of n-alcohols from a hot surface: Nukiyama and Leidenfrost temperatures

A A Mills and N F Sharrock

Physics Department, University of Leicester, Leicester LE1 7RH, England

Abstract The Nukiyama and Leidenfrost temperatures of the range of n-alcohols from methanol (C_1) to tetradecanol (C_{14}) have been investigated, and their relationships to the standard boiling points determined. The Nukiyama temperatures prove to be some 46 °C above the latter, with a further rise of only 15–18° sufficing to put an alcohol into the slowly evaporating Leidenfrost regime.

Zusammenfassung Die Nukiyama and Leidenfrost Temperaturen der Reihe der n-Alkohole von Methanol (C_1) zu Tetradekanol (C_{14}) wurden untersucht und ihre Beziehung zu den Standard Siedepunkten bestimmt. Die Nukiyama Temperaturen liegen etwa 46 °C oberhalb der letzteren, wobei eine weitere Erhöhung um 15–18 °C genügt, um einen Alkohol in das Leidenfrost-Gebiet der langsamem Verdampfung zu überführen.

1. Introduction

A previous paper (Mills and Fry 1982) explains the difference between nucleated and non-nucleated boiling of liquids upon a hot surface, defines the Nukiyama and Leidenfrost temperatures, and gives quantitative results for the homologous series of normal hydrocarbons from pentane to hexadecane. In that paper it was suggested that investigation might well be extended to the alcohols, for although the film boiling phenomenon was first observed with ethanol by Boerhaave (1732) subsequent work has been almost entirely confined to water. Although employing comparatively simple apparatus, careful technique would therefore produce useful original data relevant to industrially important materials. This research was chosen by Noëlle F Sharrock for her third-year BSc project, working with A A Mills of the academic staff.

2. Nukiyama and Leidenfrost temperatures

The lifetime of a droplet of a volatile liquid placed upon a hot surface is not a simple function of temperature, but according to Tamura and Tanasawa (1959) follows the generalised curve shown in figure 1. The liquid begins to boil at nucleated sites in the interface at a temperature T_B, and as the temperature of the hot surface is increased so the number of nucleated sites and the rate of evaporation increase, whilst the drop lifetime diminishes. However, this 'expected' behaviour does not continue indefinitely, for

above a certain temperature the droplet becomes supported by a thin film of its own vapour and, moving freely over the hot surface, takes a remarkably long time to evaporate completely. This move into a non-nucleated film boiling regime begins at point c on the curve, associated with a minimum lifetime and maximum rate of evaporation: we have called the corresponding temperature the Nukiyama temperature

Figure 1 Generalised curve of the lifetime of an evaporating droplet plotted against the temperature of the supporting surface.
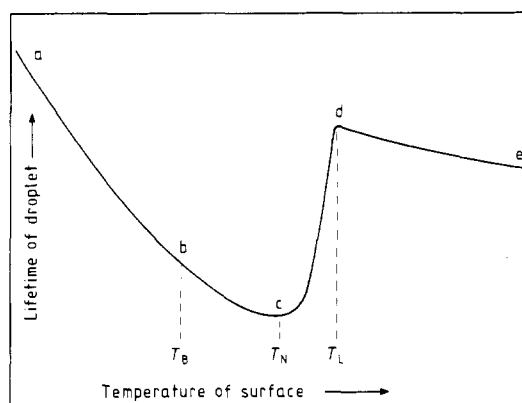
T_N (Nukiyama 1934). At point d the supporting vapour film is fully developed, the droplet is completely separated from the hot surface, and the liquid displays a minimum rate of evaporation for a temperature exceeding its normal boiling point. The associated temperature is conventionally known as the Leidenfrost temperature T_L. (A more detailed discussion is given by Mills and Fry (1982).) The Nukiyama and Leidenfrost temperatures are not fundamental properties of the liquid being heated, being obviously dependent on pressure and, to a lesser extent, the composition and finish of the hot surface.

3. Previous work

A literature search disclosed some early data for methanol and ethanol.

	Nukiyama temperature T_N (°C)	
	Methanol	Ethanol
Mosciki and Broder (1926)	94	103
Blaszkowska-Zakrzewska (1930)	—	110–115
Sauer *et al* (1938)	108–120	107–124

Boutigny (1843) obtained 134 °C for the Leidenfrost temperature T_L of ethanol.

4. Apparatus and technique

The apparatus used for the previous work on hydrocarbons was employed. It consisted of a 25 mm diameter copper disc 3 mm thick, in one face of which was turned a smooth hemispherical depression of 50 mm radius of curvature. This disc was heavily plated with gold and then polished, providing a smooth, inert metal surface with a concavity serving to retain the mobile Leidenfrost droplets. This gilded dish was supported beneath a binocular microscope upon an electrically heated silver block forming the working section of a Linkam TH 600 mineralogical heating stage. It was carefully shielded from draughts. Input power was controlled by a proportional feedback thermostat, and any preset temperature could be measured and held constant to ±0.2 °C. Calibration was carried out with standard substances of known melting point, and with an independent thermocouple.

Laboratory grade alcohols of the normal homologous series from C_1 (methanol) to C_{14} (tetradecanol) were obtained. Purity was always better than 97%. Each was freshly distilled before use, observing the boiling point T_B of the collected middle fraction. 5 μl droplets of the alcohol under test were gently dispensed into the heated concave depression of the gilded dish with a preset calibrated micropipette

('Finnpipette'). These small volumes did not cool the hot-plate appreciably, so the measurements were made under essentially isothermal conditions. Lifetimes were determined with a stopwatch, beginning when a drop left the pipette. Observation through the microscope facilitated an accurate endpoint. Five drops were timed at each temperature, cleaning the surface between each determination with a lens tissue moistened with redistilled acetone.

5. Results and discussion

The drop lifetime curve for n-pentanol is reproduced in figure 2, and is typical of the results obtained. The change of slope following soon after T_B, and the slight convexity preceding the minimum at T_N, which were first noted by Mills and Fry (1982) for hydrocarbons, are again apparent with the alcohols. In addition, an oscillating behaviour above T_L becomes obvious. This was not remarked upon by the above authors, but can be distinguished (at a low amplitude) in their curves. We therefore believe that figure 2 more nearly represents in its details the true drop lifetime curve of liquids on a hot surface.

The values of T_B, T_N and T_L obtained for the homologous series of normal alcohols are shown in table 1. The figures given for the likely errors are

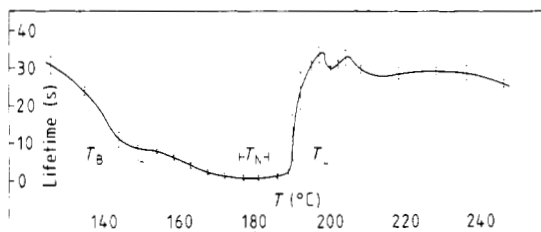**Figure 2** Drop lifetime curve for n-pentanol.

Table 1 The boiling point, Nukiyama and Leidenfrost temperatures (in °C) for the n-alcohols at atmospheric pressure.

	T_B ($\pm 1°$)	T_N	T_L
Methanol	66	111 ± 3.5	126 ± 3
Ethanol	79	126 ± 4	140 ± 3
Propanol	98	145 ± 3.5	160 ± 3.5
Butanol	120	165 ± 3.5	172 ± 3.5
Pentanol	138	180 ± 4	198 ± 3
Hexanol	158	198 ± 4	220 ± 4
Heptanol	176	220 ± 6	244 ± 4
Octanol	194	236 ± 4	254 ± 4
Nonanol	212	256 ± 4	273 ± 4
Decanol	228	272 ± 4	289 ± 3
Undecanol	244	291 ± 4	324 ± 7
Dodecanol	260	299 ± 7	324 ± 7
Tridecanol	274	324 ± 7	343 ± 7
Tetradecanol	290	343 ± 7	365 ± 7

usually equivalent to ±2–3%. Our values for T_N of methanol and ethanol correspond most nearly with those found by Sauer *et al* (1938).

Figure 3 shows plots of T_N and T_L against T_B. The graphs are linear within the experimental errors, and may be summarised by the relationships:

$$T_N = (1.01T_B + 44)\,°C$$

$$T_L = (1.02T_B + 59)\,°C.$$

In general, maximum rates of evaporation are achieved on hot surfaces maintained at $46 \pm 1\,°C$ above the standard boiling point, with a further rise of only 15–18° sufficing to put an alcohol into the slowly evaporating Leidenfrost regime.

Figure 3 Nukiyama and Leidenfrost temperatures of the n-alcohols plotted against their corresponding boiling points at atmospheric pressure.
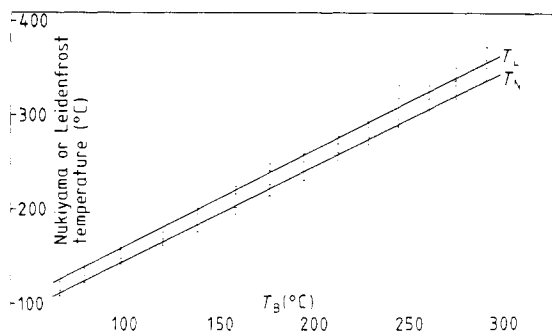
References

Blaszkowska-Zakrzewska H 1930 *Bull. Int. Acad. Pol. Sci. Lett.* **4A–5A** 188
Boerhaave H 1732 *Elementa Chemiae Lugdunum Batavorum* (Leyden) (Engl. transl. F L Curzon 1978 *Am. J. Phys.* **46** 825)
Boutigny P H 1843 *Ann. Chim. Phys.* **9** 350
Mills A A and Fry J D 1982 *Eur. J. Phys.* **3** 152
Mosciki I and Broder J 1926 *Roczn. Chem.* **6** 319
Nukiyama S 1934 *J. Soc. Mech. Eng. Japan* **37** 367 (in Japanese) (Engl. transl. S G Brickley 1960 *AERE Trans.* No 854)
Sauer E T, Cooper H B H, Akin G A and McAdams W H 1938 *Mech. Engng* **60** 669
Tamura Z and Tanasawa Y 1959 *7th Int. Symp. on Combustion* (London: Butterworths) p 509

Rate of evaporation of hydrocarbons from a hot surface: Nukiyama and Leidenfrost temperatures

A A Mills and J D Fry

Physics Department, University of Leicester, Leicester LE1 7RH, England

Abstract The Nukiyama and Leidenfrost temperatures of the range of n-alkanes from pentane to hexadecane have been investigated, and their relationships to the standard boiling points determined. The Nukiyama temperatures prove to be only some 40 °C above the latter, showing that maximum evaporation rates are produced by contact with surfaces not nearly so hot as might intuitively be expected. A temperature increase of only some 20–30 °C beyond this point is sufficient to put the hydrocarbon into the slowly-evaporating Leidenfrost regime.

Zusammenfassung Die Nukiyama und Leidenfrost Temperaturen für die n-Alkane zwischen Pentan und Hexadekan werden in ihrem Zusammenhang mit den Standardsiedepunkten bestimmt. Die Nukiyama Temperaturen liegen dabei nur etwa 40 °C oberhalb des Siedepunktes, was zeigt, daß die maximale Verdampfungsrate sich durch Kontake mit Oberflächen ergibt, die nicht annähernd so heiß sind, wie man dies intuitiv erwartet. Eine Temperaturerhöhung um etwa 20–30 °C über diesen Punkt hinaus reicht aus, um Hydrocarbone in den langsam verdampfenden Leidenfrost Bereich zu bringen.

1. Introduction

Most British university science departments now require some form of project as part of the assessment for a first degree. This period can frequently be profitably employed to allow students to become acquainted with phenomena that time does not allow to be included in lectures, and to discover for themselves that many topics are not nearly so thoroughly worked-over and understood as is commonly supposed. It is particularly satisfying if they can then reduce some of these gaps in our knowledge. An example is the evaporation of liquids other than water in the non-nucleated regime. An investigation of the behaviour of a homologous series of n-alkanes was chosen by J D Fry as his third-year project, working with A A Mills of the academic staff.

2. Nukiyama and Leidenfrost temperatures

Drops of a volatile liquid placed upon a hot surface will, of course, evaporate. However, according to Tamura and Tanasawa (1959) the lifetime of a droplet is not a simple function of temperature, but instead follows the generalised curve shown in figure 1.
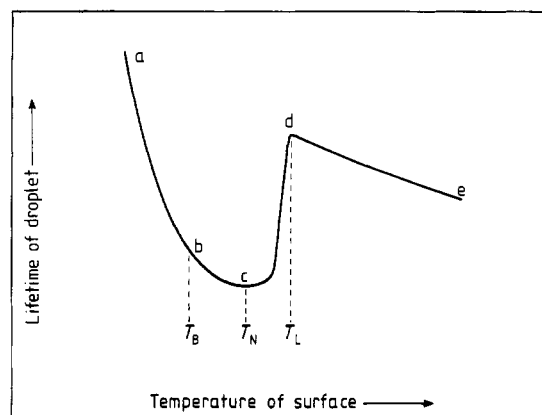

Figure 1 Generalised curve of the lifetime of an evaporating droplet versus temperature of the supporting surface.

When the temperature of the surface is below that corresponding to the normal boiling point of the liquid at the ambient pressure, the droplet either wets the surface and spreads out or, more commonly, assumes a plano-convex shape. It evaporates slowly and quietly along section a–b of figure 1.

At the boiling point T_B tiny vapour bubbles begin to appear at nucleated sites in the liquid/solid interface. The number of these sites, and consequently the rate of evaporation, increases with temperature along section b–c until, by the time c is reached, the lens-shaped droplet has been replaced by a violently boiling irregular mass. The rapid vaporisation occurring at a multitude of nucleated sites produces a hissing sound.

However, a comparatively small increase, to point d, in the temperature of the heated surface exerts a profound effect. The liquid gathers itself into flattened globules which, supported by a cushion of their own vapour, glide above the hot surface. This move into a non-nucleated, film-boiling regime is accompanied by a dramatic fall in the rate of evaporation, and constitutes the well-known Leidenfrost effect (Wares 1966, Bell 1967, Curzon 1978).

It will be seen that the *maximum* rate of evaporation (minimum lifetime; point c) is associated with a temperature which we propose to call the Nukiyama temperature T_N after its discoverer (Nukiyama 1934). This appears to us to be preferable to the rather ambiguous term 'crisis boiling point', especially as that temperature (above the normal boiling point) corresponding to a *minimum* rate of evaporation (point d) is already conventionally known as the Leidenfrost temperature T_L. The transitional section (c–d) of the curve is sometimes unstable and hard to define experimentally, but above T_L the levitated spheroids can be remarkably stable and reproducible along curve d–e. A very large temperature increase (typically some hundreds of degrees) is necessary before the overall rate of evaporation again approaches that observed at the Nukiyama temperature. Similar considerations apply to spillages of liquefied petroleum gases and cryogenic fluids boiling below ambient temperatures.

Nukiyama's observations on the related changes in heat flux from a hot wire or tube entirely submerged in a boiling liquid were confirmed and extended by subsequent workers, as detailed by Drew and Mueller (1937) and McAdams (1954). In more recent years considerable progress has been made in the understanding and theoretical prediction of the Leidenfrost phenomenon (Gottfried *et al* 1966, Baumeister and Simon 1973, Michiyoshi and Makino (1978). However, the Nukiyama temperatures of liquids other than water have received very little attention. This is surprising in view of the fact that evaporation of organic liquids (and especially petroleum hydrocarbons) is such an important process in modern technology. We have therefore examined the range of straight-chain alkanes from pentane to hexadecane.

3. Apparatus and technique

A shallow spherical depression of 50 mm radius of curvature was turned in a 25 mm diameter copper disc 3 mm thick, and smoothed with successively finer grades of diamond paste. A heavy coating (about 10 μm) of pure gold was then electroplated upon the copper, and the resulting surface highly polished. This produced a smooth, inert metal surface unaffected by the temperatures and materials used in the experimental runs. This gilded dish was supported beneath a binocular microscope upon an electrically heated silver block forming the working section of a Linkam TH 600 mineralogical heating stage. It was carefully shielded from draughts. Input power was controlled by a proportional feedback thermostat, and any preset temperature could be measured and held constant to ±0.2 °C. Calibration was carried out with standard substances of known melting point, and with an independent thermocouple.

The purity of the hydrocarbons employed was better than 99%, and they were freshly distilled before use, observing the boiling point T_B of the collected middle fraction. Drops of the liquid under test were gently dispensed into the heated concave depression with a microlitre syringe, a standard all-glass syringe fitted with various needles, or a dropper pipette. These gave reproducible droplets varying between 6 and 13 μl for a given hydrocarbon. These small volumes did not cool the hotplate appreciably, so the measurements were made under essentially isothermal conditions. Lifetimes were determined with an electronic stopwatch, beginning when a drop left the syringe needle. Observation through the microscope facilitated an accurate endpoint. Five drops were timed at each temperature, except around the Nukiyama and Leidenfrost temperatures where measurements on ten drops were made. The standard error of the mean lifetime was always less than 4%.

4. Results and discussion

The curve for n-octane is reproduced in figure 2, and is typical of the results obtained. The shape of the curve proved independent of droplet size over the range employed, the effect of changing volume being simply one of displacement of the entire curve along a vertical axis. The slight convexity about halfway between T_B and T_N is not mentioned by Tamura and Tanasawa, but is not thought to be an artefact because it also appears on the curves for the other hydrocarbons. The extension of the Leidenfrost curve towards lower temperatures was
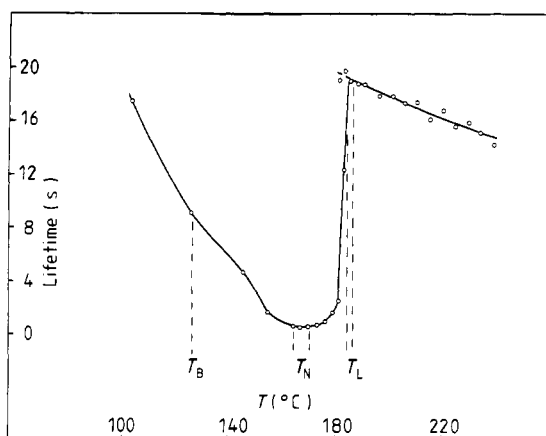
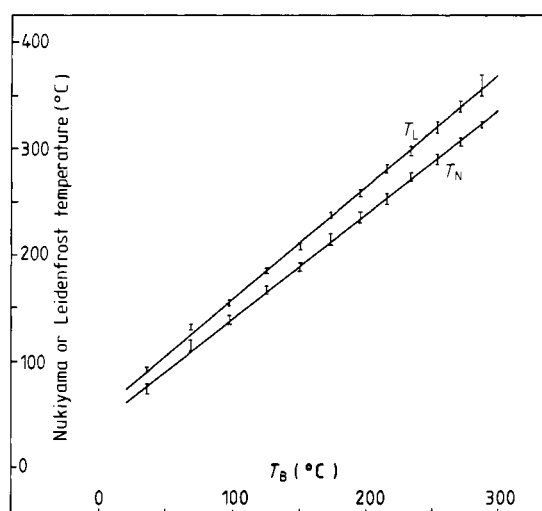**Figure 2** Drop lifetime curve for n-octane.

Figure 3 Nukiyama and Leidenfrost temperatures of the n-alkanes plotted against their corresponding boiling points at normal atmospheric pressure.

$$T_N = (0.98T_B + 42)\,°C$$
$$T_L = (1.06T_B + 52)\,°C$$

Table 1 The boiling point, Nukiyama and Leidenfrost temperatures (degrees centigrade) for the n-alkanes at atmospheric pressure.

n-alkane	T_B	T_N	T_L
Pentane	36	70–78	90–93
Hexane	69	110–120	130–135
Heptane	98	135–143	152–156
Octane	126	164–170	184–186
Nonane	151	185–192	206–210
Decane	174	210–220	235–240
Undecane	195.5	230–240	255–260
Dodecane	216	248–258	278–285
Tridecane	234	270–278	294–302
Tetradecane	253.5	286–294	315–325
Pentadecane	270.5	303–309	335–345
Hexadecane	287	320–325	350–370

5. Possible application and extension

From our experience we can recommend this investigation as suitable for undergraduate projects, as it gives experience in searching a fair body of literature; in careful (yet comparatively simple) experimental technique; and in consideration of errors. It demonstrates some unusual facets of the phenomenon of boiling, and it will be apparent that original investigations could readily be made by extension to other organic liquids, for example the alcohols.

obtained if the droplets were pre-warmed before allowing them to fall upon the heated surface. The transitional section between T_N and T_L became less abrupt and more stable, and so easier to measure and define, as the boiling point of the liquid increased.

The broken lines in figure 2 indicate the uncertainties associated with the numerical values assigned to the Nukiyama and Leidenfrost temperatures (see table 1). It will be seen that for n-octane T_L is the better defined, but it was observed that the position tended to reverse with decreasing volatility of the hydrocarbon. This behaviour is reflected in the lengths of the error bars shown in the plots of T_B versus T_N and T_L in figure 3. The graphs are linear within the experimental error, and may be summarised by the relationships:

References
Baumeister K J and Simon F F 1973 *J. Heat Transfer* **95** C 166
Bell K J 1967 *Chem. Eng. Prog. Symp. Ser.* 63 **79** 73
Curzon F L 1978 *Am. J. Phys.* **46** 825
Drew T B and Mueller A C 1937 *Trans. Am. Inst. Chem. Eng.* **33** 449
Gottfried B S, Lee C J and Bell K J 1966 *J. Heat and Mass Transfer* **9** 1167
McAdams W H 1954 *Heat Transmission* (New York: McGraw-Hill)
Michiyoshi I and Makino K 1978 *J. Heat and Mass Transfer* **21** 605
Nukiyama S 1934 *J. Soc. Mech. Eng. Japan* **37** 367 (In Japanese) (Engl. transl. S G Brickley 1960 *AERE Trans.* No 854)
Tamura Z and Tanasawa Y 1959 *7th Int. Symp. on Combustion* (London: Butterworths) p 509
Wares C 1966 *J. Heat and Mass Transfer* **9** 1153

A boiling heat transfer paradox

G. Guido Lavalle, P. Carrica, V. Garea,[a] and M. Jaime

Centro Atómico Bariloche and Instituto Balseiro, Comisión Nacional de Energía Atómica, 8400 Bariloche, Argentina

An instructive experiment for observing the Leidenfrost phenomenon is presented. The experiment, suitable for an undergraduate experimental course, consists of introducing a copper body at room temperature into liquid nitrogen and observing its temperature history. The experiment is then repeated with the body covered by a thermal insulating material, observing that the body reaches thermal equilibrium much more rapidly in the second case. This apparent paradox greatly motivates the students, who need to understand the different regimes of boiling heat transfer to resolve it. The paper also contains an approximate method to determine the insulator thickness that gives the minimum cooling period.

I. INTRODUCTION

Boiling heat transfer is widely used in engineering applications and is often encountered in physics laboratories. The research in this area began with the works of H. Boerhaave[1] and J. G. Leidenfrost.[2] In 1756 the latter published "A Tract About Some Qualities of Common Water," where he presented some experiments consisting of letting small drops of water evaporate on hot iron surfaces. He found that when the surface was glowing, it took more than 30 s for the drops to evaporate, but when the surface became cooler it took only about 9 or 10 s. Such a paradoxical effect is due to the existence, in the first case, of a vapor film between the drop and the iron which greatly reduces the heat transport and hence retards the evaporation. The experiment has been repeated more recently by different authors[3,4] and similar effects have been observed in a variety of situations, some of which are described in Ref. 1.

Heat transfer involving vapor formation at a vertically oriented heated wall is usually divided into different boiling regimes according to the manner in which vapor is generated. Consider a stagnant liquid in thermodynamic equilibrium with its vapor at a given pressure. The temperature of the liquid will henceforth be referred to as saturation temperature. If the wall temperature is raised above that of the liquid, a first regime will be observed for small wall–liquid temperature difference in which no vapor is generated at the wall. The heat flux is transported by superheated liquid which rises to the free liquid–gas interface, because of buoyancy forces, where it evaporates (see Fig. 1, regime I).

When the wall temperature is increased bubbles are formed at the wall that depart and rise through the liquid. This mechanism of heat transfer is called "nucleate boiling" and is characterized by a steep increase of heat flux with the wall superheat as can be seen in Fig. 1 (regime II). The nucleate boiling regime exists up to a point called the maximum-heat-flux, critical-heat-flux, or "burnout" point (point A in Fig. 1). The name "burnout" comes from the fact that when the heat flux is controlled and is raised above this point, the wall temperature jumps to point B in Fig. 1, which usually corresponds to thousands of degrees. These temperatures are above the melting point of the commonly used heater materials and thus the heater "burns out."

The wall temperature jump appears because a vapor film completely covers the heater and "insulates" it. This heat transfer regime is called "film boiling" (regime IV).

If the wall temperature is now decreased the temperature difference decreases to a point called "minimum-heat-flux" or Leidenfrost point (C, Fig. 1), where the vapor film is no longer stable. If the controlled variable is the heat flux the heater will experience a sudden decrease in temperature, corresponding to a jump to point D in the figure. If the independent variable is the wall temperature, a third regime is encountered between the maximum and minimum heat fluxes in which both nucleate and film boiling coexist alternately. This regime is called transition boiling (region III) and was apparently first described by Drew and Mueller.[5]

The curve displayed in Fig. 1 is called the pool-boiling or Nukiyama characteristic curve, in honor of S. Nukiyama[6] who first obtained it after carrying out experiments with an electrically heated platinum wire immersed in water at saturation temperature. The curve is usually shown as log–log because of the wide ranges of variation of temperature and heat flux.
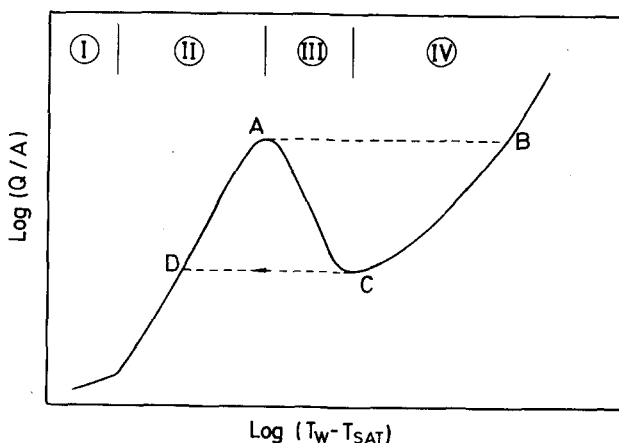

Fig. 1. Typical pool boiling curve showing the different regimes of heat transfer: I: natural convection, II: nucleate boiling, III: transition boiling, and IV: film boiling.

II. EXPERIMENTAL METHOD

One of the simplest ways of measuring the characteristic boiling curve consists of introducing a hot body into the liquid at its saturation temperature. If the temperature difference between the body and the liquid is high enough, the film boiling regime IV will be established.

The body will cool down, rather slowly due to the low heat transfer rates, and Leidenfrost point C will be reached. The vapor film will then break off while the heat flux progressively increases as transition boiling regime III is established.

The body will cool further and the nucleate boiling regime II will be encountered. After this the heat transfer will be accomplished by natural convection currents (regime I) and finally thermal equilibrium will be attained.

From a record of the temperature history the heat flux may be calculated, at least approximately, and thus the boiling curve may be constructed by the following procedure.

It is assumed that the temperature gradients within the body are small. This is a good approximation if the Biot number

$$Bi = hL/K \tag{1}$$

is small[7] (typically around or below unity), where L is the body's characteristic length, K is the thermal conductivity of the material, and h is the surface heat-transfer coefficient, which is defined as

$$h = \frac{Q/A}{T_W - T_{SAT}}, \tag{2}$$

where Q is the heat transferred from the body to the liquid per unit time, A is the surface area, T_W is the wall temperature, and T_{SAT} is the saturation temperature of the liquid at the working pressure.

The smallness of the Biot number indicates that the temperature is nearly uniform within the body, corresponding to a situation in which the thermal resistance of the body, measured by L/K, is small compared with the resistance for the heat to flow to the fluid $1/h$. In such a case the temperature difference between any two points of the body is small compared with the difference between the surface and the fluid temperatures.

The problem is that the surface heat-transfer coefficient is not known *a priori* and does not even remain constant throughout the experiment. It would not depend on wall temperature if there existed a linear relationship between Q/A and $T_W - T_{SAT}$, which is certainly not the case in boiling heat transfer as can be seen from Fig. 1.

Nonetheless it is assumed that the Biot number is small during the cool down; it will be calculated *a posteriori* to assess the validity of this assumption.

Under this hypothesis, the temperature at any point of the body is approximately equal to the wall temperature and to the mean temperature:

$$T = T_W = \overline{T}, \tag{3}$$

where the mean temperature is defined as

$$\overline{T} = \int T\, dV \Big/ \int dV \tag{4}$$

in which dV is the element of volume and the integrals should be performed over the entire body.

It is thus possible to write the heat balance equation:

$$\frac{Q}{A} = \frac{V\rho c}{A} \frac{dT}{dt}, \tag{5}$$

where V is the volume of the body, ρ is its density, c the specific heat (temperature-dependent), and t the time.

Therefore, a calculation can be performed to obtain the instantaneous heat flux per unit area measuring the temperature history and knowing the physical properties and geometrical parameters of the body. The plot of this quantity against the instantaneous temperature gives the characteristic boiling-curve of the wall–liquid pair under analysis.

The experiment just described is quite classical. It has been performed by Merte and Clark[8] to obtain boiling curves under different gravity conditions and has been reported more recently by Listerman et al.[9] as an intermediate level undergraduate laboratory experiment.

The main experiment reported here consists of recording the temperature history of the same body but covered with a thin layer of a thermal insulating material. Again, energy conservation requires that the heat transferred from the body to the insulator equal the heat transferred to the fluid plus the variation of the internal energy of the insulator.

If the variation of the energy stored in the insulator can be neglected and the insulator thickness e is very small compared with the characteristic length of the body, the equation of conduction of heat in the thin thermal insulating layer is reduced to that of heat conduction in a slab:[10]

$$Q/A = \int_{T_b}^{T_a} K_I/e\, dT, \tag{6}$$

where K_I is the thermal conductivity of the insulating material and T_a and T_b are the temperatures at the inner and outer surface of the insulating layer, respectively. If the body covered by the thin insulating layer is a sphere of radius r_a, and r_b ($= r_a + e$) is the external radius of the spherical shell formed by the insulator the heat transfer rate is given by[11]

$$Q\left(\frac{1}{r_a} - \frac{1}{r_b}\right) = 4\pi \int_{T_b}^{T_a} K_I\, dT = 4\pi \overline{K}_I (T_a - T_b), \tag{7}$$

where $\overline{K}_I$ is the mean conductivity over the range of temperature from T_b to T_a and the last equation is its definition.

If the temperature of the body is measured, the rate of heat flowing from the hot body may be calculated with Eq. (5). Equations (6) or (7) may then be used to calculate the temperature at the outer surface of the insulator assuming that the temperature at the inner surface equals that of the body.

III. EXPERIMENTAL DETAILS

In the experiment presented here the body was a copper sphere of 25.4 mm in diameter and the working fluid was liquid nitrogen at atmospheric pressure. A chromel–constantan thermocouple was located at the center of the sphere. The chromel–constantan pair was selected because it provides a large voltage compared with other pairs and thus the resolution of the temperature measurement is increased, which is important when the heat flux is to be obtained. The thermocouple was inserted through a 1.5-mm-diam hole and a small amount of solder was added to ensure a good thermal contact. The reference junction was placed in an ice bath and the resulting voltage was mea-

sured with a Hewlett-Packard 3455 digital voltometer with an IEEE-488 interface. The digital signal was recorded by an Apple II + computer. Data were acquired at a rate of 1 reading every 0.185 s and stored on magnetic media for off-line analysis.

To insulate the sphere the method favored by long-distance swimmers was used: a layer of grease was applied. Instead of lanolin, Apiezon type-N grease was used. This was selected because it has a known thermal conductivity,[12] which is three orders of magnitude smaller than that of copper.[13] The thickness of the grease layer was calculated by measuring the applied volume and assuming the uniformity of the layer. While the uniformity was checked visually no anomalous vapor generation at any location was noticed, an observation made possible because the experiments were performed in a transparent Dewar vessel.

The experiment may be further simplified if it is to be performed in an undergraduate physics laboratory. The results presented below may be obtained replacing the grease by a covering made of paper or teflon tape. However, in this case the results should be considered as being of a qualitative nature because heat transfer across the tape is greatly influenced by the air trapped in between. Another interesting variation is to measure the derivative of the temperature signal with an analog circuit and to send this signal and that of the temperature itself to an X-Y recorder. Thus the Nukiyama curve is automatically obtained. Nevertheless the plot is again not of quantitative use because the variation of the specific heat with temperature is not taken into account.

In the present work a fourth-order polynomial was fitted to the copper-specific-heat versus temperature data[14] to calculate the heat transfer. The temperature derivative was computed numerically using a three-point scheme with variable step.[15] This algorithm provides a smooth curve and does not flatten the peak-heat-flux, because the time step selected by the program is the smallest one when the temperature is rapidly varying and is larger otherwise.

The validity of the assumption concerning the temperature gradients within the body may be assessed by placing more thermocouples at different locations in the body. In particular, a thermocouple may be positioned near the surface and connected in opposition with the centered one.[8]

IV. EXPERIMENTAL RESULTS

Results of the measurements carried out with the bare sphere are shown in Figs. 2 and 3. In Fig. 2(a), curve (I), the temperature-versus-time plot shows the typical form for this kind of experiment, while Fig. 2(b) shows the evolution of the heat flux. During the first part of the cooling film boiling regime IV exists and the positive concavity indicates that the heat flux is diminishing as the temperature is decreasing. The change in concavity (at approximately 185 s) corresponds to minimum-heat-flux point C and indicates the beginning of the transition-boiling regime III. The second inflection point (at approximately 194 s) corresponds to the peak-heat-flux at A. From that moment on nucleate-boiling regime II is established and finally thermal equilibrium is attained. The natural convection regime I could not be distinguished in the present experiments. The characteristic pool-boiling curve for liquid nitrogen is constructed by plotting the heat flux against the temperature difference between the body and the liquid
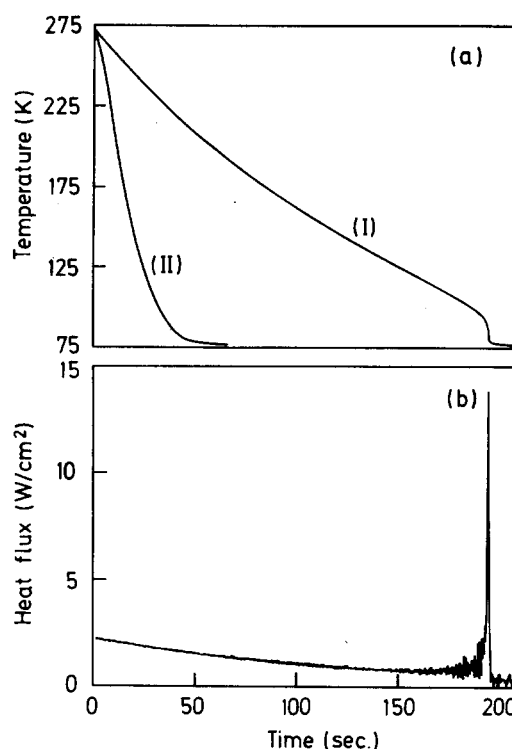

Fig. 2. (a) Experimental cooling curves of a 25.4-mm-diam copper sphere (I) in liquid nitrogen and of the same sphere covered by a 0.3 mm of Apiezon N grease (II). (b) Heat flux corresponding to the bare sphere calculated with Eq. (5).

(Fig. 3). This experimental curve is in good agreement with previously reported data.[16]

The Biot number may now be evaluated. To obtain a conservative estimate the values of the heat flux per unit area and wall superheat are taken at the point of the peak heat flux $[(Q/A)_{PHF} = 13.8$ W/cm^2, $(T_W - T_{SAT})_{PHF} = 6.2$ K], thus obtaining a value of 0.51 for the maximum Biot number, based on the sphere radius. Therefore, the approximations already made were reasonable.[17]

Figure 2, curve (II), shows the temperature history of the copper sphere covered by a grease layer 0.3 mm thick. From the graph it becomes clear that the insulated body cools down much more rapidly than the bare one. Defining
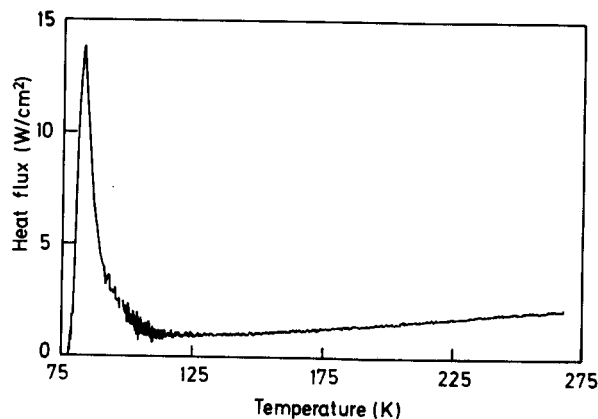

Fig. 3. Experimental pool boiling curve corresponding to the bare copper sphere.

the cooling period as the time required for the body to cool from 273 to 78 K, its value is 196 s for the bare body and only 48 s for the grease-covered body. This is what is herein called the "boiling heat transfer paradox."

The paradox is resolved in terms of the different boiling heat-transfer modes. The wall temperature of the bare sphere is sufficiently high to give rise to the film-boiling regime. This is the cause of a small heat flux which in turn leads to a slow decay of the temperature. Thus the vapor film remains stable for a long period of time. When the film collapses the heat transfer is greatly increased (note that the peak heat-flux is one order of magnitude greater than that of the minimum-heat-flux) and the sphere rapidly reaches the temperature of the nitrogen.

When the insulation is present the temperature measured can no longer be considered as being equal to the surface temperature. Considering the very small thermal conductivity of the grease, a steep temperature gradient exists within it. The surface temperature may be calculated by means of Eqs. (6) or (7) with the heat flux obtained from the copper heat balance, Eq. (5). If the wall temperature is low enough it causes the heat transfer to be in the transition- or nucleate-boiling regime. If this is the case the heat flux is greatly increased and the cooling period is shortened, which resolves the apparent paradox. In fact, the explanation of the experimental results is the same as that of the Boerhaave–Leidenfrost phenomenon, where liquid droplets were found to evaporate very slowly when the heated surface was hot enough to be in the film-boiling regime.

The system may be studied further. Since the temperature drop within the grease depends on the layer thickness it is expected that if the layer is too thin, the surface temperature will not be low enough to cause the transition- or nucleate-boiling regime to exist, thus lengthening the cooling period. On the other hand, once the nucleate boiling exists from the beginning of the quenching a further increase in insulator thickness will again result in an increase of the cooling period.

This behavior is clearly observed in Fig. 4, where the temperature-versus-time curve is shown for different grease thicknesses. Curve (a) corresponds to the bare sphere and the others to insulated-body experiments. Curve (b) was obtained with a layer of 0.025 mm thick. It can be seen clearly that the collapse of the vapor film occurs

earlier than in the bare case. With increasing insulation thickness [curve (c): 0.1 mm, (d): 0.2 mm], the temperature drop within the grease is larger, the transition occurs earlier and thus the cooling period is shortened.

Such behavior continues up to the point when the peak-heat-flux is attained from the beginning of the experiment. Further increments of insulation cause the heat transfer to be in the nucleate-boiling regime throughout the cooling, and with thicker layers of grease the initial heat flux decreases due to lower wall temperatures.

Therefore, a critical thickness of insulation may be defined as being that necessary to cause the surface temperature to equal the temperature corresponding to the peak-heat-flux of the bare body when it is at its initial temperature. Using Eq. (7) and with the parameters of the present experiment [inner surface temperature: $T_a = 273$ K, $T_{PHF} = 83$ K, $Q/A_{PHF} = 13.8$ W/cm^2, sphere radius: $r_a = 1.27$ cm, grease mean thermal conductivity: $\bar{K} = 0.2$ W/(mK)] it yields a value of external radius of $r_b = 1.298$ cm, which is equivalent to a critical thickness of $e = 0.28$ mm. Approximately this value was used in the experiment of curve (e), $e = 0.3$ mm, in Fig. 4 and should be considered an estimation of the thickness which gives the minimum cooling period. The calculation is not exact since a shorter cooling time may be obtained by beginning in the transition regime and reaching the peak-heat-flux a moment later. This is the case for curve (f) ($e = 0.25$ mm), which begins with a lower cooling rate than that of the previous curve, but then the heat transfer rate is increased and results in a shorter cooling period.

As expected, a thicker layer of grease yields larger cooling periods [curve (g): 0.5 mm, (h): 0.75 mm].

The behavior in the complete range of experienced thicknesses is shown in Fig. 5 in a cooling-period versus thickness-of-insulation plot. The minimum is clearly seen and agrees fairly well with the above-defined critical value.

It should be noted that the present definition of critical insulator thickness has nothing in common with the classical critical radius of insulation which gives the maximum-heat-flux due to an increase in the heat transfer area.[18]

Finally, it is worth noting that, given a pair of fluid-insulator materials, the critical thickness depends on the temperature of the body. The cause of this is that a thicker layer of insulator is needed to force the wall temperature to be at the peak condition if the body temperature is larger.
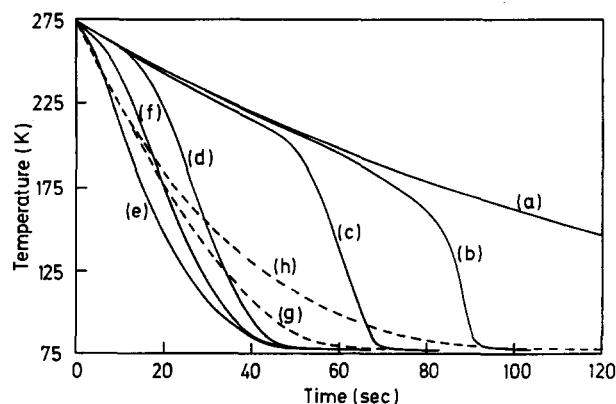

Fig. 4. Cooling curves of the sphere covered by different grease thicknesses [(a): bare, (b): 0.025 mm, (c): 0.1 mm, (d): 0.2 mm, (e): 0.3 mm, (f): 0.25 mm, (g): 0.5 mm, (h): 0.75 mm].
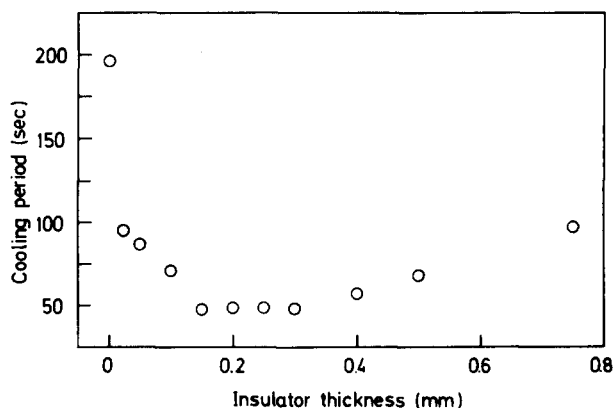

Fig. 5. Time required for the sphere to cool from 273 to 78 K as a function of thickness of insulation. The first point from the left corresponds to the bare-body experiment.

V. CONCLUSIONS

It was shown that adding an insulating layer to an object that is to be cooled in a much colder fluid causes the cooling to be more rapid. This effect was demonstrated with a simple experiment, suitable for an undergraduate experimental course, and is due to the fact that the insulation causes the surface temperature to be lower. This, in turn, causes an anticipated change of boiling heat-transfer mode, from film to transition or nucleate regime, and the subsequent increase in heat flux which shortens the cooling period.

A critical thickness of insulation was defined which approximately gives the thickness of minimum cooling period. It was found to be in good agreement with the experimental data.

[a] Current address: Rensselaer Polytechnic Institute, Troy, NY 12180-3590.

[1] See the citation in F. L. Curzon, "The Leidenfrost phenomenon," Am. J. Phys. **46**, 825–828 (1978).

[2] J. G. Leidenfrost, "On the fixation of water in diverse fire," translated by Mrs. C. Wares, Int. J. Heat Mass Trans. **9**, 1153–1166 (1966).

[3] B. S. Gottfried, C. J. Lee, and K. J. Bell, "The Leidenfrost phenomenon: film boiling of liquid droplets on a flat plate," Int. J. Heat Mass Trans. **9**, 1167–1187 (1966).

[4] J. Walker, "The amateur scientist," Sci. Am. **237**, 126–130 (1977).

[5] T. B. Drew and A. C. Mueller, "Boiling," Trans. AIChE **33**, 449–454 (1937).

[6] S. Nukiyama, "Maximum and minimum values of heat transmitted from metal to boiling water under atmospheric pressure," J. Soc. Mech. Eng. Jpn. **37**, 367–374 (1934).

[7] W. M. Rohsenow and H. Y. Choi, *Heat, Mass and Momentum Transfer* (Prentice-Hall, Englewood Cliffs, NJ, 1961), pp. 110–119.

[8] H. Merte, Jr. and J. A. Clark, "Boiling heat transfer with cryogenic fluids at standard, fractional and near-zero gravity," J. Heat Trans. **86**, 351–359 (1964).

[9] T. W. Listerman, T. A. Boshinski, and L. F. Knese, "Cooling by immersion in liquid nitrogen," Am. J. Phys. **54**, 554–558 (1986).

[10] H. S. Carslaw and J. C. Jaeger, *Conduction of Heat in Solids* (Oxford U. P., Oxford, 1980), 2nd ed., pp. 92–93.

[11] Reference 10, pp. 230–231.

[12] T. Ashworth, J. E. Loomer, and M. M. Kreitman, "Thermal conductivity of nylons and Apiezon greases," Adv. Cryog. Eng. **18**, 271–279 (1972).

[13] *Thermophysical Properties of Matter*, Y. S. Touloukian, Director (IFI-/Plenum, New York, 1972), Vol. 1, p. 81.

[14] *A Compendium of the Properties of Materials at Low Temperature (Phase 1), Part 2: Properties of Solids*, edited by V. J. Johnson (WADD Technical Report 60-56, Ohio, 1960), p. 4.122-1.

[15] F. B. Hildebrand, *Introduction to Numerical Analysis* (McGraw-Hill, New York, 1956), p. 134.

[16] J. A. Clark, "Cryogenic heat transfer," Adv. Heat Trans. **5**, 325–517 (1968).

[17] Due to the variation of the heat transfer coefficient throughout the experiment, the temperature difference between the center and the surface of the sphere cannot be obtained analytically. In Ref. 8 a maximum temperature difference of approximately 1 K is reported for a similar experiment.

[18] Reference 8, pp. 103–104.

The Liénard–Wiechert potential and the retarded shape of a moving sphere

J. M. Aguirregabiria, A. Hernández, and M. Rivas

Física Teórica, Facultad de Ciencias, Universidad del País Vasco, Apdo 644, 48080 Bilbao, Spain

The subtleties in the derivation of the retarded Liénard–Wiechert potential for a point charge are stressed by explicitly computing and drawing the retarded shape of a moving sphere. This shape is the effective integration region for the charge density and it is computed, with the aid of the "information collecting sphere," in the limit of vanishing radius (or, equivalently, from the point of view of a remote observer).

I. INTRODUCTION

The retarded scalar potential $\phi(P,T)$, created at time T and position P by a charge density distribution $\rho(\mathbf{r},t)$, is given by[1]

$$\phi(P,T) = \frac{1}{4\pi\epsilon_0} \int \frac{\rho(\mathbf{r}, T - R/c)}{R} dV. \qquad (1)$$

Here, R is the retarded distance from P to the point $\mathbf{r}$ at which the source was located at the retarded time $t = T - R/c$.

In the case of a point charge moving with constant velocity v, for given values of P and T the retarded distance R has a single value, say R_0, over the whole charge and the corresponding potential can be written as

$$\phi(P,T) = \frac{1}{4\pi\epsilon_0 R_0} \int \rho\left(\mathbf{r}, T - \frac{R}{c}\right) dV. \qquad (2)$$

One is then tempted to substitute the total charge q for the integral appearing in the last expression. This, however, would give us an incorrect result. By using the correct value for that integral, namely

$$\int \rho\left(\mathbf{r}, T - \frac{R}{c}\right) dV = \frac{q}{(1 - \beta \cos \theta)}, \qquad (3)$$

one gets the Liénard–Wiechert potential:

© 1992 American Association of Physics Teachers   597